AMERICAN SOCIETY FOR MICROBIOLOGY | mBio

Virology | Research Article

CD4 downregulation precedes Env expression and protects HIV-1-infected cells from ADCC mediated by non-neutralizing antibodies

Jonathan Richard,[1,2] Gérémy Sannier,[1,2] Li Zhu,[3] Jérémie Prévost,[1,2] Lorie Marchitto,[1,2] Mehdi Benlarbi,[1,2] Guillaume Beaudoin-Bussières,[1,2] Hongil Kim,[3] Yaping Sun,[3] Debashree Chatterjee,[1] Halima Medjahed,[1] Catherine Bourassa,[1] Gloria-Gabrielle Delgado,[1] Mathieu Dubé,[1] Frank Kirchhoff,[4] Beatrice H. Hahn,[5,6] Priti Kumar,[3] Daniel E. Kaufmann,[7,8,9] Andrés Finzi[1,2]

AUTHOR AFFILIATIONS See affiliation list on p. 16.

ABSTRACT HIV-1 envelope glycoprotein (Env) conformation substantially impacts antibody-dependent cellular cytotoxicity (ADCC). Envs from primary HIV-1 isolates adopt a prefusion "closed" conformation, which is targeted by broadly neutralizing antibodies (bnAbs). CD4 binding drives Env into more "open" conformations, which are recognized by non-neutralizing Abs (nnAbs). To better understand Env–Ab and Env–CD4 interaction in CD4+ T cells infected with HIV-1, we simultaneously measured antibody binding and HIV-1 mRNA expression using multiparametric flow cytometry and RNA flow fluorescent *in situ* hybridization (FISH) techniques. We observed that *env* mRNA is almost exclusively expressed by HIV-1 productively infected cells that already downmodulated CD4. This suggests that CD4 downmodulation precedes *env* mRNA expression. Consequently, productively infected cells express "closed" Envs on their surface, which renders them resistant to nnAbs. Cells recognized by nnAbs were all *env* mRNA negative, indicating Ab binding through shed gp120 or virions attached to their surface. Consistent with these findings, treatment of HIV-1-infected humanized mice with the ADCC-mediating nnAb A32 failed to lower viral replication or reduce the size of the viral reservoir. These findings confirm the resistance of productively infected CD4+ T cells to nnAbs-mediated ADCC and question the rationale of immunotherapy approaches using this strategy.

IMPORTANCE Antibody-dependent cellular cytotoxicity (ADCC) represents an effective immune response for clearing virally infected cells, making ADCC-mediating antibodies promising therapeutic candidates for HIV-1 cure strategies. Broadly neutralizing antibodies (bNAbs) target epitopes present on the native "closed" envelope glycoprotein (Env), while non-neutralizing antibodies (nnAbs) recognize epitopes exposed upon Env–CD4 interaction. Here, we provide evidence that *env* mRNA is predominantly expressed by productively infected cells that have already downmodulated cell-surface CD4. This indicates that CD4 downmodulation by HIV-1 precedes Env expression, making productively infected cells resistant to ADCC mediated by nnAbs but sensitive to those mediated by bnAbs. These findings offer critical insights for the development of immunotherapy-based strategies aimed at targeting and eliminating productively infected cells in people living with HIV.

KEYWORDS HIV-1, ADCC, Env, nnAbs, bNAbs, hu-mice, A32, RNA-flow fish

Highly active antiretroviral therapy (ART) efficiently suppresses HIV-1 replication and significantly increase the life expectancy of people living with HIV-1 (PLWH) (1, 2). However, it has become evident that even lifelong ART cannot eradicate the virus. Viral reactivation and rebound can occur upon treatment interruption due to the presence

Invited Editor Diane L. Bolton, United States Military HIV Research Program, Silver Spring, Maryland, USA

Editor Ronald Swanstrom, The University of North Carolina at Chapel Hill, Chapel Hill, North Carolina, USA

Address correspondence to Andrés Finzi, andres.finzi@umontreal.ca, Daniel E. Kaufmann, daniel.kaufmann@chuv.ch, or Priti Kumar, priti.kumar@yale.edu.

Jonathan Richard, Gérémy Sannier, and Li Zhu contributed equally to this article. Author order was determined in order of increasing seniority.

The authors declare no conflict of interest.

Received 14 June 2024
Accepted 16 September 2024
Published 7 October 2024

of a latent reservoir, persisting mainly in long-lived memory CD4+ T cells (3–6). New approaches aimed at eradicating or functionally curing HIV-1 infection by targeting and eliminating productively or latently infected cells are needed. Monoclonal antibodies (mAbs) are attractive therapeutics for HIV cure strategies, since they target virus-specific antigens and have the potential to harness host immune responses such as antibody-dependent cellular cytotoxicity (ADCC). The HIV-1 envelope glycoprotein (Env) is the only viral antigen that is present on the surface of HIV-1-infected cells, thus representing the main target for immunotherapy-based strategies (7, 8). In recent years, several clinical trials explored broadly neutralizing antibodies (bnAbs) as therapeutic agents to reduce the HIV-1 reservoir via Fc-mediated effector functions (9). Monotherapy or a combination of bnAbs targeting multiple regions of the Env trimer, including the V3 glycan supersite (10–1074, PGT121), the V2 apex (PGDM 1400, CAP256-VRC26), or the CD4 binding site (CD4bs) (3BNC117, N6, VRC01, VRC07-523), are currently under investigation. Administration of bnAbs to humans has been found to be safe and effective in lowering viremia and maintaining viral suppression for varying periods of time after treatment interruption (10–16). However, recent data suggest that bnAbs may not be as broad and/or effective as predicted, in part because of circulating viruses with pre-existing resistance to the administered bnAbs (9). So-called "non-neutralizing" Abs (nnAbs) have been evaluated as a potential alternative because some of them target highly conserved Env epitopes that are usually occluded in the "closed" trimer, including the coreceptor-binding site (CoRBS) (17–19), the inner domain of gp120 (20–22) or the gp41 immunodominant domain (23). These nnAbs are naturally elicited during HIV-1 infection and can mediate potent Fc effector functions (23–29).

HIV-1 Env is a conformationally flexible molecule that transitions from an unliganded "closed" State 1 to an "open" CD4-bound State 3 conformation (30–32) upon CD4 interaction. Envs from most primary HIV-1 isolates adopt a "closed" conformation that is efficiently targeted by bnAbs, but is resistant to nnAbs (30, 33–37), which target epitopes that are occluded within the unliganded "closed" trimer. Env interaction with CD4 or small CD4-mimetic compounds are known to induce more "open" conformations, thus sensitizing infected cells to ADCC mediated by CD4-induced (CD4i) nnAbs (24, 25, 27, 28, 34, 35, 37–43). To avoid exposing these nnAb epitopes, the Env trimer is stabilized by multiple intermolecular interactions, including between the V1, V2, and V3 variable loops as well as the gp120 β20–β21 element, which maintain a "closed" conformation (32, 44, 45). In addition, HIV-1 expresses the accessory proteins Nef and Vpu, which indirectly modulate Env conformation by downregulating CD4 from the surface of infected cells, thus preventing a premature Env–CD4 interaction that would otherwise result in the exposure of CD4i Env epitopes (24, 27). Vpu-mediated counteraction of the restriction factor BST-2 (also named "tetherin"), known to tether viral particles at the surface of infected cells, also reduces cell-surface levels of Env (24, 27, 46, 47).

Despite advances in understanding Env–Ab and Env–CD4 interactions, the capacity of nnAbs to target and eliminate productively infected cells by ADCC remain controversial. Several studies reported that cells infected with primary viruses expressing functional Vpu and Nef proteins are resistant to ADCC mediated by CD4i nnAbs, because they maintain surface-expressed Env in a "closed" conformation (24, 25, 28, 33–43, 48, 49). Other studies report that CD4i nnAbs can mediate ADCC responses, but they have used infectious molecular clones (IMCs) that are defective for Nef expression (50–61). These IMCs contain reporter genes (e.g., the *Renilla* luciferase [LucR] gene) upstream of the *nef* gene, which significantly reduces Nef expression and thus CD4 downregulation from the surface of infected CD4+ target cells. The resulting premature Env–CD4 interaction promotes artificial exposure of otherwise occluded CD4i epitopes (40, 62, 63).

Here, we used multiparametric flow cytometry and RNA flow fluorescent *in situ* hybridization (FISH) techniques to characterize cell populations targeted by bNAbs and nnAbs in the context of primary CD4+ T cell infection. We show that *env* mRNA is specifically detected among cells that already downmodulated cell-surface CD4, which renders these cells refractory to recognition by nnAbs. Although some CD4+ cells are

bound by nnAbs, they are all negative for *env* mRNA, indicating that they are not productively infected, and nnAbs binding is mediated through the recognition of shed gp120 and/or viral particles coated at their cell surface. Similar results were obtained with *ex vivo*-expanded CD4+ T cells isolated from PLWH. Finally, the ADCC-mediating nnAb A32 failed to reduce HIV-1 replication and the size of the viral reservoir in a humanized mouse model (hu-mice) that supports Fc-effector functions. These findings raise questions about curative immunotherapy-based strategies that rely solely on nnAbs, specifically those targeting CD4i epitopes.

MATERIALS AND METHODS

The materials and methods have been previously described in references 25, 27, 28, 34, 39, 42, 43, 64–66. They are summarized here for the convenience of the reader.

Cell lines and primary cells

The 293T human embryonic kidney cells (obtained from ATCC) were maintained at 37°C under 5% CO_2 in Dulbecco's modified Eagle medium (Wisent, St. Bruno, QC, Canada), supplemented with 5% fetal bovine serum (VWR, Radnor, PA, USA) and 100 U/mL of penicillin/streptomycin (Wisent). Human peripheral blood mononuclear cells (PBMCs) from HIV-negative and HIV-positive individuals obtained by leukapheresis and Ficoll-Paque density gradient isolation were cryopreserved in liquid nitrogen until further use. CD4+ T lymphocytes were purified from resting PBMCs by negative selection using immunomagnetic beads per the manufacturer's instructions (StemCell Technologies, Vancouver, BC) and were activated with phytohemagglutinin-L (10 µg/mL) for 48 h and then maintained in RPMI 1640 (Thermo Fisher Scientific, Waltham, MA, USA) complete medium supplemented with rIL-2 (100 U/mL).

Antibody production

FreeStyle 293 F cells (Thermo Fisher Scientific) were grown in FreeStyle 293F medium (Thermo Fisher Scientific) to a density of 1×10^6 cells/mL at 37°C with 8% CO_2 with regular agitation (150 rpm). Cells were transfected with plasmids expressing the light and heavy chains of each mAb using ExpiFectamine 293 transfection reagent, as directed by the manufacturer (Thermo Fisher Scientific). One week later, the cells were pelleted and discarded. The supernatants were filtered (0.22-µm-pore-size filter), and antibodies were purified by protein A affinity columns, as directed by the manufacturer (Cytiva, Marlborough, MA, USA).

HIV-1 studies in humanized mice

NSG-15 mice with expression of the human IL15 gene in the NOD/ShiLtJ background were purchased from the Jackson Laboratory (Bar Harbor, ME, USA). The mice were bred and maintained under specific pathogen-free conditions. All animal studies were performed with authorization from the Institutional Animal Care and Use Committees (IACUC) of Yale University. NSG-15-Hu-PBL mice were engrafted as described (42). Briefly, 3.5×10^6 PBMCs, purified by Ficoll density gradient centrifugation of healthy donor blood buffy coats (obtained from the New York Blood Bank) were injected IP in a 200-µL volume into 6- to 8-week-old NSG-15 mice, using a 1-cm^3 syringe and a 25-gauge needle. Cell engraftment was tested 15 days post-transplant. Then, 100 µL of blood was collected by retroorbital bleeding. PBMCs were isolated by Ficoll density gradient centrifugation; stained with fluorescently labeled anti-human CD45 (BD Biosciences, Cat#: 555485), CD3 (Biolegend, Cat#: 300424), CD4 (Biolegend, Cat#: 317432), CD8 (BD Biosciences, Cat#: 561617), and CD56 (Biolegend, Cat#: 362508) antibodies; and analyzed by flow cytometry to confirm engraftment. Humanized mice were intraperitoneally challenged with 30,000 PFU of HIV-1_{JRCSF}. Infection profile was analyzed routinely by retro-orbital bleeding and flow cytometric analysis of peripheral blood for human immune cells and

plasma viral load (PVL) analysis. For flow cytometry, 100 µL of blood was collected by retro-orbital bleeding at each time point. PBMCs were isolated by Ficoll density gradient centrifugation, and cells were stained with Fluor-conjugated antibodies as detailed above. PVL was measured at day 5, 8, and 11 post-infection, while HIV-1 reservoirs were measured at day 11 post-infection as previously described (42).

Plasmids and proviral constructs

Transmitted/Founder (T/F) IMC of patient CH077 was inferred and constructed as previously described (67). The generation of *nef*-defective CH077TF was previously described and consists in the introduction of premature stop codons in the *nef* reading frame using site-directed mutagenesis protocol (68). The CH077TF D368R was also generated by site-directed mutagenesis as previously described (43). Proviral constructs comprising an HIV-1 NL4.3-based isogenic backbone engineered for the insertion of heterologous *env* strain sequences and expression in *cis* of full-length Env (Env–IMCs) were previously described (69). The Env–IMCs utilized in the present study are those encoding Env from BaL (pNL-B.BaL.ecto), CH040 (pNL-B.CH040.ecto), CH058 (pNL-B.CH058.ecto), SF162 (pNL-B.SF162.ecto). or YU2 (pNL-B.YU-2.ecto). The proviral plasmid pNL4.3 was used as control (70). The vesicular stomatitis virus G (VSV-G)-encoding plasmid was previously described (71).

Viral production, infections, and *ex vivo* amplification

For *in vitro* infection, vesicular stomatitis virus G (VSV-G)-pseudotyped HIV-1 viruses were produced by co-transfection of 293T cells with an HIV-1 proviral construct and a VSV-G-encoding vector using the calcium phosphate method. Two days post-transfection, cell supernatants were harvested, clarified by low-speed centrifugation (300 × *g* for 5 min), and concentrated by ultracentrifugation at 4°C (100,605 × *g* for 1 h) over a 20% sucrose cushion. Pellets were resuspended in fresh RPMI, and aliquots were stored at −80°C until use. Viruses were then used to infect activated primary CD4+ T cells from healthy HIV-1-negative donors by spin infection at 800 × *g* for 1 h in 96-well plates at 25°C. Viral preparations were titrated directly on primary CD4+ T cells to achieve similar levels of infection among the different IMCs tested (approximately 10% of p24+ cells). To expand endogenously infected CD4+ T cells, primary CD4+ T cells obtained from PLWH were isolated from PBMCs by negative selection. Purified CD4+ T cells were activated with PHA-L at 10 µg/mL for 48 h and then cultured for at least 6 days in RPMI 1640 complete medium supplemented with rIL-2 (100 U/mL) to reach greater than 10% infection for the ADCC assay.

Antibodies

The following anti-Env Abs were used to stain HIV-1-infected primary CD4+ T cells: anti-gp41 F240; anti-cluster A A32, C11; anti-coreceptor binding site 17b; anti-gp120 outer domain 2G12, anti-CD4 binding site VRC03, 3BNC117; anti-V3 glycan PGT121, PGT126, 10–1074; anti-V2 apex PG9; anti-gp120-gp41 interface PGT151. The HIV-IG polyclonal antibody consists of anti-HIV immunoglobulins purified from a pool of plasma from asymptomatic PLWH (NIH AIDS Reagent Program). Goat anti-human IgG (H + L) (Thermo Fisher Scientific) pre-coupled to Alexa Fluor 647 was used as secondary antibodies in flow cytometry experiments. Rabbit antisera raised against Nef (NIH AIDS Reagent Program) was used as primary antibodies in intracellular staining. Brillant Violet 421 (BV421)-conjugated donkey anti-rabbit antibodies (Biolegend) was used as secondary antibodies to detect Nef antisera binding by flow cytometry. Fluorescein isothiocyanate (FITC)- or phycoerythrin (PE)-conjugated mouse anti-human CD4 (clone OKT4; Biolegend) was used for cell-surface staining of HIV-1-infected primary CD4+ T cells, while PE- or FITC-conjugated mouse anti-HIV-1 p24 (clone KC57; Beckman Coulter) was used for intracellular staining.

Flow cytometry analysis of cell-surface staining

Cell surface staining was performed at 48 h post-infection. Mock- or HIV-1-infected primary CD4+ T cells were incubated for 30 min at 37°C with anti-Env mAbs (5 µg/mL) or HIV-IG (50 µg/mL). Cells were then washed once with phosphate-buffered saline (PBS) and stained with the appropriate Alexa Fluor 647-conjugated secondary antibody (2 µg/mL) for 20 min at room temperature. Cells were then stained with FITC- or PE-conjugated mouse anti-CD4 Abs. After two PBS washes, cells were fixed in a 2% PBS–formaldehyde solution. Infected cells were then permeabilized using the Cytofix/Cytoperm Fixation/Permeabilization Kit (BD Biosciences, Mississauga, ON, Canada) and stained intracellularly using PE- or FITC-conjugated mouse anti-p24 mAb (clone KC57; Beckman Coulter, Brea, CA, USA; 1:100 dilution). The percentage of infected cells (p24+) was determined by gating on the living cell population according to a viability dye staining (Aqua Vivid; Thermo Fisher Scientific). Alternatively, cells were stained intracellularly with rabbit antisera raised against Nef (1:1,000) followed by BV421-conjugated anti-rabbit secondary antibody. Samples were acquired on an LSR II cytometer (BD Biosciences), and data analysis was performed using FlowJo v10.5.3 (Tree Star, Ashland, OR, USA).

Antibody-dependent cellular cytotoxicity (ADCC) assay

Measurement of ADCC using a fluorescence-activated cell sorting (FACS)-based infected cell elimination (ICE) assay was performed at 48 h post-infection. Briefly, HIV-1-infected primary CD4+ T cells were stained with AquaVivid viability dye and cell proliferation dye eFluor670 (Thermo Fisher Scientific) and used as target cells. Cryopreserved autologous PBMC effector cells, stained with cell proliferation dye eFluor450 (Thermo Fisher Scientific), were added at an effector:target ratio of 10:1 in 96-well V-bottom plates (Corning, Corning, NY). Anti-Env mAbs (5 µg/mL) was added to appropriate wells, and cells were incubated for 5 min at room temperature. The plates were subsequently centrifuged for 1 min at 300 × *g*, and incubated at 37°C, 5% CO_2 for 5 h before being stained with FITC- or PE-conjugated mouse anti-CD4 Abs. After one PBS wash, cells were fixed in a 2% PBS–formaldehyde solution. Infected cells were then permeabilized using the Cytofix/Cytoperm Fixation/Permeabilization Kit (BD Biosciences, Mississauga, ON, Canada) and stained intracellularly using PE- or FITC-conjugated mouse anti-p24 mAb (clone KC57; Beckman Coulter, Brea, CA, USA; 1:100 dilution). Productively infected cells were identified based on p24 and CD4 detection as described above. Samples were acquired on an LSR II cytometer (BD Biosciences), and data analysis was performed using FlowJo v10.5.3 (Tree Star). The percentage of ADCC was calculated with the following formula: [(% of $CD4^{low}p24^{high}$ cells in Targets plus Effectors) − (% of $CD4^{low}p24^{high}$ cells in Targets plus Effectors plus plasma or mAbs) / (% of $CD4^{low}p24^{high}$ cells in Targets) × 100] by gating on live target cells.

RNA flow-FISH analysis

All buffers and fixation reagents were provided with a kit, with the exception of flow cytometry staining buffer (2% FCS/PBS). The HIV-1 RNA flow-FISH assay was performed as previously described and as per manufacturer's instructions (64–66). Briefly, cells were harvested 48 h post-infection and stained with the anti-Env mAbs A32 or PGT126 as described above. Cells were then stained with Fixable Viability Dye (20 min, 4°C, Fixable LiveDead, eBioscience) and then with a mix containing a brilliant stain buffer (BD Biosciences) and the surface markers for CD4+ T cell detection (CD3 and CD4) and CD8/NK/B cells and macrophage exclusions (CD8, CD56, CD19, CD16) (30 min, 4°C). Samples were fixed, permeabilized with buffers provided by the manufacturer, and labeled intracellularly for the structural HIV-1 p24 protein with the anti-p24 clone KC57 antibody (30 min RT followed by 30 min 4°C, Beckman Coulter). HIV-1 RNA probing was performed using PrimeFlow RNA Assay (ThermoFisher). HIV-1 RNA was labeled using HIV-1 *env* RNA (Thermofisher; catalog number VF6-6000978) and HIV-1 *nef* RNA

(Thermofisher; catalog number (VF4-6000647) probe sets. HIV-1 *env* RNA was designed based on CH077TF full *env* sequence, whereas HIV-1 *nef* RNA was based on consensus B HIV-1 sequence. Each probeset allows the hybridization of specific complementary branched DNA nanostructure with different excitation/emission spectra. The probeset was diluted 1:5 in diluent and hybridized to the target mRNAs for 2 h at 40°C. Samples were washed to remove excess probes and stored overnight in the presence of RNAsin. Signal amplification was achieved by performing sequential hybridization with DNA branches (i.e., Pre-Amplifier and Amplifier). The first DNA branch in the Pre-Amplifier Mix was added at a 1:1 ratio and was allowed to hybridize for 1.5 h at 40°C. Then the second DNA branch in the Amplifier Mix was added and hybridized for 1.5 h at 40°C (64–66). Amplified mRNAs were labeled with fluorescently tagged probes allowing hybridization for 1 h at 40°C. Samples were acquired on an LSRFortessa (BD Biosciences) and analyzed using FlowJo (BD, V10.7.0). Unspecific binding of the fluorescent-labeled branched probe in the multiplex kit can lead to a low level of false-positive background noise, which, if present, is detected across all the four channels corresponding to the types of labeled probes (AF488, AF594, AF647, AF750). To decrease background noise, we thus left the AF594 channel vacant and excluded false-positive events based on fluorescence in this channel before further gating. Gates were set on the HIV-uninfected donor control or unstimulated control where appropriate.

Statistical analysis

Statistics were analyzed using GraphPad Prism version 9.1.0 (GraphPad, San Diego, CA, USA). Every data set was tested for statistical normality, and this information was used to apply the appropriate (parametric or nonparametric) statistical test. P values < 0.05 were considered significant; significance values are indicated as *P < 0.05, **P < 0.01, ***P < 0.001, ****P < 0.0001.

RESULTS

Expression of CD4, p24, and Nef defines recognition of HIV-1-infected CD4+ T cells by nnAbs and bnAbs

To characterize cell populations targeted by nnAbs and bnAbs in HIV-1-infected primary CD4+ T cells, we used multiparametric flow cytometry to simultaneously probe CD4 and viral protein expression. Activated primary CD4+ T cells were mock infected or infected with the transmitted-founder virus CH077 (CH077TF). Two days post-infection, cells were stained with a panel of nnAbs and bnAbs, followed by appropriate secondary Abs. Cells were then stained for cell-surface CD4 prior to staining for intracellular HIV-1 p24. Given that the *nef* gene is abundantly expressed during the early phase of the HIV-1 replication cycle (72, 73), we also evaluated the expression of this accessory protein by intracellular staining as previously described (62). The different cell populations were gated based on cell-surface CD4 and intracellular p24 detection as shown in Fig. 1A. As expected, uninfected $CD4^{high}p24^{-}$ cells were not recognized by bnAbs of various specificities (PGT126, PG9, 3BNC117, PGT151, and 2G12) (Fig. 1B through D) (Table 1). Interestingly, this population was efficiently recognized by CD4i nnAbs targeting the coreceptor-binding site (17b) or the gp120 inner domain (A32, C11) as well as a pool of purified immunoglobulins from PLWH (HIV-IG). However, the $CD4^{high}p24^{-}$ cells were not recognized by the CD4i gp41-specific nnAbs F240. The absence of binding by bnAbs and F240 suggested that these cells were likely coated with shed gp120 rather than presenting CD4-bound cell-surface Env trimer. This is in line with previous work showing that uninfected CD4+ T cells expose CD4i epitopes on their cell surface after interacting with gp120 shed from productively infected cells within the same culture (34, 74, 75). Indeed, introduction of a CD4bs (D368R) mutation into CH077TF that prevents Env–CD4 interaction (18, 24, 76), abrogated the recognition of the $CD4^{high}p24^{low}$ population by all gp120-specific nnAbs tested (Fig. S1A and B).

In addition to productively infected CD4+ T cells, which efficiently downregulated CD4 ($CD4^{low}p24^{high}$), we identified a subset of $CD4^{high}p24^{low}$ cells, as previously

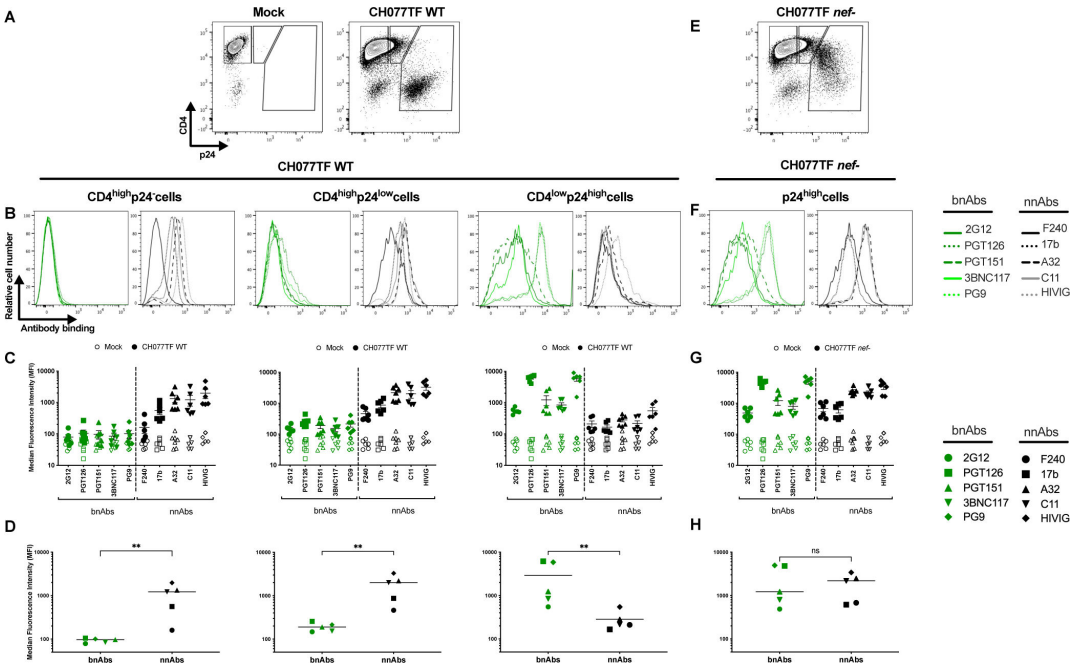

FIG 1 Recognition of HIV-1-infected primary CD4+ T cells by bnAbs and nnAbs. Primary CD4+ T cells, mock infected or infected with the transmitted-founder virus CH077, either wild type (WT) or defective for Nef expression (*nef*-), were stained with a panel of bnAbs and nnAbs, followed with appropriate secondary Abs. Cells were then stained for cell-surface CD4 prior to detection of intracellular HIV-1 p24. (A, E) Example of flow cytometry gating strategy based on cell-surface CD4 and intracellular p24 detection. (B, F) Histograms depicting representative staining with bnAbs (green) and nnAbs (black). (C, G) Graphs shown represent the median fluorescence intensities (MFI) obtained for at least six independent staining with the different mAbs. Error bars indicate means ± standard errors of the means. (D, H) Graphs shown represent the mean MFI obtained with each mAb. Statistical significance was tested using Mann–Whitney U test (**P < 0.01; ns, non-significant).

reported (52, 59, 77–81). This $CD4^{high}p24^{low}$ subset was efficiently recognized both by the gp120-specific nnAbs and HIV-IG, but was resistant to bnAbs binding (Fig. 1B and D). This population was also recognized by the gp41-specific F240 nnAb, suggesting the presence of trimeric Env bound to CD4. However, recognition of the $CD4^{high}p24^{low}$ cells by CD4i nnAbs was substantially reduced upon the introduction of the D368R mutation (Fig. S1A and B). This mutation also specifically reduced the proportion of $CD4^{high}p24^{low}$ cells (Fig. S1C). These findings, along with the observation that these cells do not express Nef (Fig. 2), suggest that $CD4^{high}p24^{low}$ cells are not productively infected, but contain CD4–Env complexes on their surface resulting from the binding of shed gp120 and/or viral particles.

As expected, cells that expressed a high level of p24 ($CD4^{low}p24^{high}$) were poorly recognized by nnAbs (Fig. 1B through D). We reasoned that this was because they efficiently downregulated cell-surface CD4, which precludes premature Env triggering, and thus prevents the exposure of normally occluded epitopes (24, 27, 34). $CD4^{low}p24^{high}$ cells also expressed Nef (Fig. 2) and were efficiently recognized by bnAbs, known to preferentially recognize Env in its "closed" conformation (Fig. 1B through D). However, when we used a *nef*-defective virus, these cells were efficiently recognized by nnAbs (Fig. 1E through H), in agreement with previous observations (8, 27, 34, 38, 40, 62, 82).

To test whether our findings extend to IMCs widely used in the ADCC field (29, 36, 54, 56, 77, 81, 83–85), we infected primary CD4+ T cells with viruses produced from a pNL4.3 backbone expressing different Envs, including BaL and NL4.3. As shown in Fig. S2A and B, the patterns of bnAbs and nnAbs binding were very similar to those observed for CH077TF. The $CD4^{high}p24^{-}$ and $CD4^{high}p24^{low}$ cell populations were preferentially recognized by the nnAbs, while the $CD4^{low}p24^{high}$ cells were efficiently targeted by the bnAbs. Interestingly, despite similar levels of productive infection ($CD4^{low}p24^{high}$, Fig.

TABLE 1 Antibody specificity

Antibody	Epitope
bnAbs	
2G12	Outer domain of gp120
PGT121	V3 glycan supersite
PGT126	V3 glycan supersite
10–1074	V3 glycan supersite
PGT151	gp120-gp41 interface
3BNC117	CD4-binding site
VRC03	CD4-binding site
PG9	V2 apex
nnAbs	
F240	gp41 immunodominant region
17b	Coreceptor binding site
19b	V3 crown
A32	gp120 inner domain
C11	gp120 inner domain

S2C), an enrichment of the $CD4^{high}p24^{low}$ population was detected in the context of infection with the NL4.3 and BaL Envs compared to Envs from primary viruses (CH058TF, CH040TF, SF162, and YU2) (Fig. S2D). The reasons for this are unclear but may be due to greater gp120 shedding of the tier 1 NL4.3 and BaL Env.

Taken together, our results indicate that cells recognized by nnAbs express high levels of CD4, are either $p24^{low}$ or $p24^{-}$, and are negative for Nef expression. In contrast, bnAbs recognize cells that efficiently downregulate CD4 and express a high level of p24 and Nef proteins.

env mRNA is predominantly detected in cells that already downregulated CD4

To better understand the underlying mechanisms behind the differential recognition of infected cells by bNAbs versus nnAbs, we used a previously described RNAflow cytometric fluorescence *in situ* hybridization (RNA flow-FISH) method (64–66). This method identifies productively infected cells by detecting cellular HIV-1 mRNA using *in situ* RNA hybridization and intracellular Ab staining for the HIV-1 p24 protein. In the context of these experiments, *env* and *nef* mRNA probes were used to identify productively infected CD4+ T cells. Briefly, primary CD4 T cells were mock infected or infected with the CH077TF IMC. Two days post-infection, cells were stained for surface CD4 before fixation and permeabilization to enable detection of the HIV-1 p24 antigen and HIV-1 mRNAs. Cell populations were first defined based on their cell-surface CD4 and intracellular p24 co-expression, as presented in Fig. 3A. Productively infected cells were identified as *nef* mRNA+/*env* mRNA+. The vast majority of cells with detectable cell-surface CD4 ($CD4^{high}p24^{-}$ or $CD4^{high}p24^{low}$) were negative for HIV-1 mRNA (Fig. 3A and B), while cells that efficiently downmodulated CD4 ($CD4^{low}p24^{low}$ and $CD4^{low}p24^{high}$) were enriched for *nef* and *env* mRNA transcripts (Fig. 3A and B; Fig. S3). When gating on productively infected cells based on *nef* and *env* mRNA detection, we confirmed that the $CD4^{low}p24^{high}$ cells represent the major source of productively infected cells (Fig. 3C and D). These results show that *env* mRNA is predominantly expressed by HIV-1-infected cells that already downregulated CD4 ($CD4^{low}p24^{low}$ and $CD4^{low}p24^{high}$) (Fig. S3). This analysis also captured stages of infection ($CD4^{low}p24^{low}$), where CD4 is already downmodulated, while *env* mRNA expression intensifies, suggesting that CD4 downmodulation precedes *env* mRNA expression.

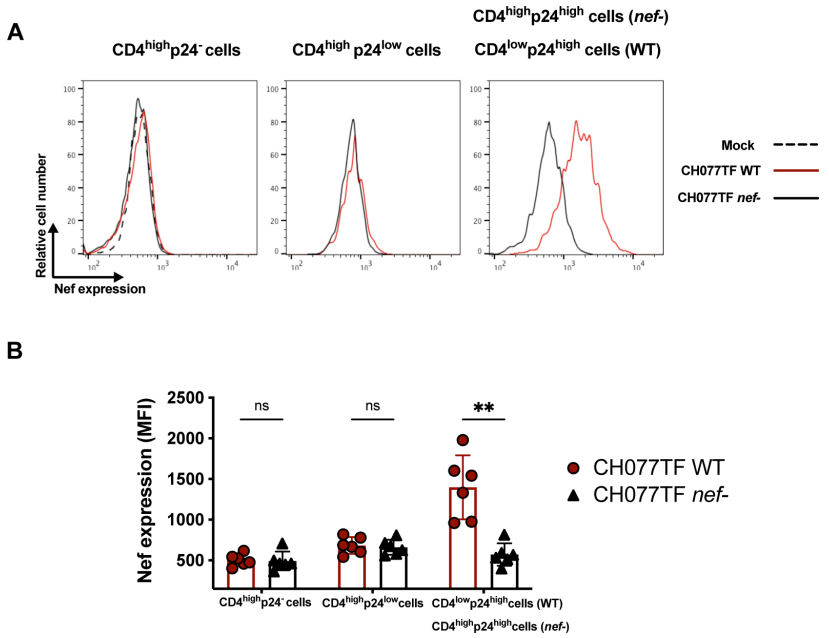

FIG 2 Nef is expressed in HIV-1-infected cells undergoing CD4 downregulation and expressing high levels of p24. Primary CD4+ T cells, mock infected or infected with the transmitted-founder virus CH077, either WT or defective for Nef expression (*nef-*) were stained for cell-surface CD4 prior to detection of intracellular HIV-1 p24 and Nef expression. (A) Histograms depicting representative intracellular Nef staining when gating on $CD4^{high}p24^{-}$, $CD4^{high}p24^{low}$, or $CD4^{low}p24^{high}$ cells. In the context of cells infected with CH077TF *nef-*, in the absence of Nef-mediated CD4 downmodulation, the $p24^{high}$ remained $CD4^{high}$ ($CD4^{high}p24^{high}$). (B) Quantification of the median fluorescence intensities (MFI) obtained for six independent experiments. Error bars indicate means ± standard errors of the means. Statistical significance was tested using multiple Mann–Whitney tests with a Holm–Sidak post-test (**$P < 0.01$; ns, non-significant).

Cells targeted by A32 are negative for HIV-1 mRNA

We next combined flow cytometry and RNA flow-FISH methods to compare the capacity of nnAbs and bnAbs to bind productively infected cells. Mock- or CH077TF-infected primary CD4 T cells were first stained with the nnAb A32 or the bNAb PGT126. Cells were then stained for cell-surface CD4 detection, intracellular p24, and HIV-1 mRNAs. Productively infected cells were identified based on the simultaneous detection of *nef* and *env* mRNA transcripts (Fig. 4A). As shown in Fig. 4B and C, productively infected cells (*env*/*nef* mRNA+ cells) were recognized by PGT126, but not by A32. In contrast, *env*/*nef* mRNA– cells were targeted by A32, but not by PGT126. Similar results were obtained when cells were classified by Ab recognition (Fig. 4D through F; Fig. S4), with the majority of PGT126+ cells co-expressing HIV-1 mRNA. In contrast, cells recognized by A32 were negative for *env* and *nef* mRNA (Fig. 4D through F; Fig. S4). These results indicate that cells targeted by A32 do not express *env* mRNA (Fig. S4), are not productively infected, and thus are likely coated with gp120 and/or viral particles. The observation that not all HIV-1 mRNA+ cells are recognized by PGT126 could be attributed to cells in an early stage of infection, where *env* is expressed, but the viral protein has not yet reached the cell surface. Supporting this interpretation, the $CD4^{low}p24^{low}$ that have already downmodulated CD4 and positive for *nef* and *env* mRNA were not efficiently recognized by either PGT126 or A32 (Fig. S5).

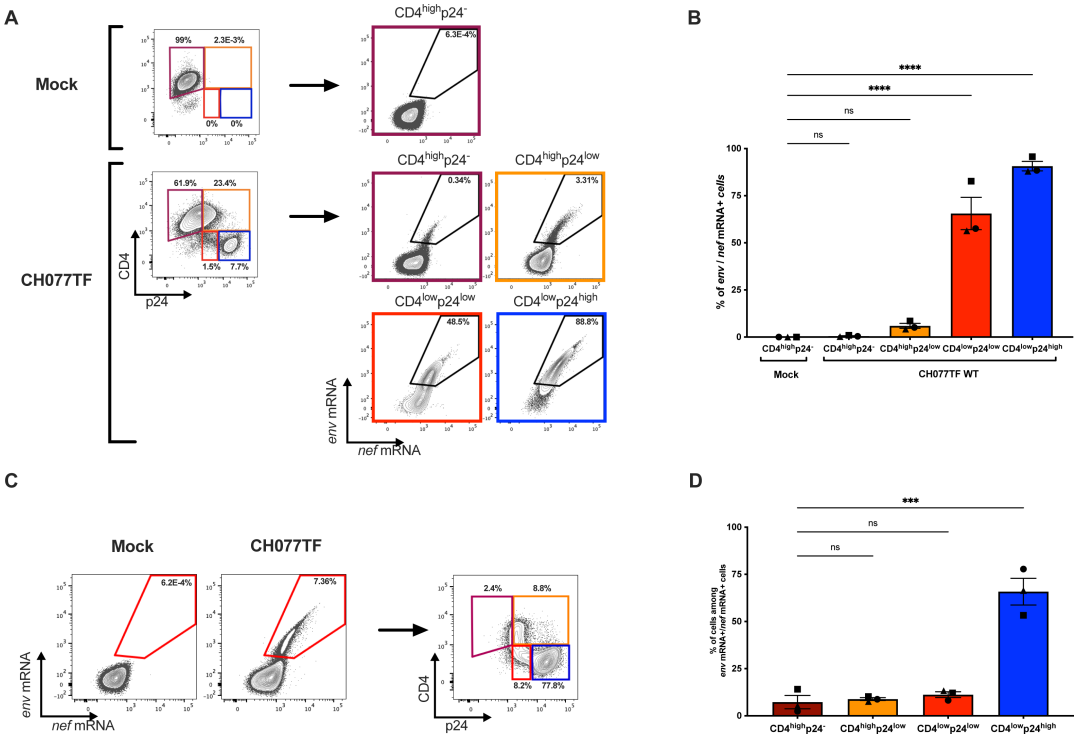

FIG 3 HIV-1 late transcripts are mostly detected among cells that downregulated CD4. Purified primary CD4+ T cells, mock infected or infected with the transmitted-founder virus CH077 WT, were stained for cell-surface CD4 prior to detection of intracellular HIV-1 p24 and *env* mRNA and *nef* mRNA by RNA flow-FISH. (A) Representative example of flow cytometry gating strategy based on cell-surface CD4 and intracellular p24 detection and representative example of RNA flow-FISH detection of *env* and *nef* mRNA among the different cell populations. (B) Quantification of the percentage of *env* mRNA+ *nef* mRNA+ cells detected among the different cell populations in three different donors. (C) Alternatively, productively infected cells were first identified based on *env* and *nef* mRNA detection (D) Quantification of the percentage of $CD4^{high}p24^{-}$, $CD4^{high}p24^{low}$, $CD4^{low}p24^{low}$, and $CD4^{low}p24^{high}$ cells among the *env* and *nef* mRNA+ cells with three different donors. Statistical significance was tested using one-way analysis of variance (ANOVA) with a Holm–Sidak post-test (****P < 0.0001; ns, non-significant).

Ex vivo expanded CD4+ T cells isolated from PLWH are resistant to ADCC responses mediated by nnAbs

Our results indicated that productively infected cells are principally $CD4^{low}p24^{high}$, express *nef* and *env* mRNA, and are not recognized by nnAbs. To confirm these findings with primary clinical samples, we expanded CD4+ T cells from PLWH. Briefly, CD4+ T cells were isolated from six chronically infected individuals and activated *ex vivo* using PHA-L/IL-2 (25, 39, 41). CD4+ T cells from people without HIV were used as controls. Viral replication was monitored over time by intracellular p24 staining (Fig. 5A). Upon expansion, CD4+ T cells were stained with a panel of bnAbs and nnAb (Table 1), followed by the appropriate secondary Abs. Cells were stained for cell-surface CD4 prior to the detection of intracellular HIV-1 p24 and Nef proteins (Fig. 5B; Fig. S6). Consistent with the results obtained with IMC infections (Fig. 2), productively infected $CD4^{low}p24^{high}$ cells were the only ones that were also positive for the Nef protein (Fig. S6). These cells were efficiently recognized by bnAbs and largely resistant to nnAbs binding (Fig. 5C through E). In contrast, nnAbs mainly recognized $CD4^{high}$ cells that were either $p24^{-}$ or $p24^{low}$ as well as negative for Nef expression (Fig. 5C through E; Fig. S6). To evaluate the susceptibility of productively infected cells to ADCC responses mediated by bnAbs and nnAbs, expanded endogenously infected cells were used as target cells and autologous peripheral blood mononuclear cells (PBMCs) as effectors using a FACS-based ADCC assay (Fig. 6). Consistent with antibody binding, productively infected $CD4^{low}p24^{high}$ cells were resistant to ADCC mediated by nnAbs, but sensitive to those mediated by bnAbs.

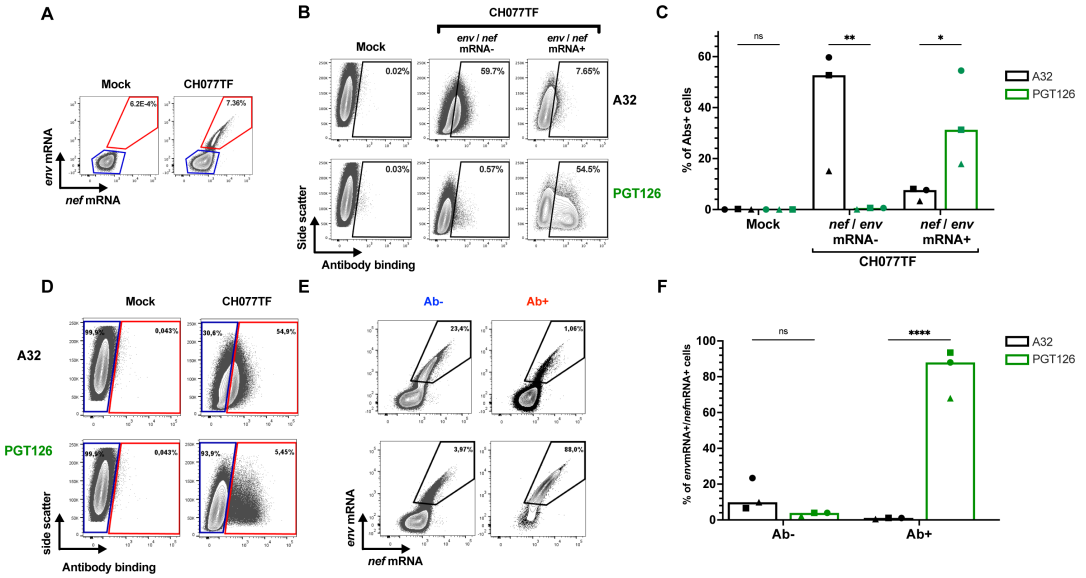

FIG 4 Productively infected cells are resistant to recognition by A32. Purified primary CD4+ T cells, mock infected or infected with the transmitted-founder virus CH077 WT, were stained with A32 or PGT126, followed with appropriate secondary Abs. Cells were then stained for cell-surface CD4 prior to detection of intracellular HIV-1 p24 and *env* mRNA and *nef* mRNA by RNAflow FISH. (A–C) In a first analysis, HIV-infected cells were identified, then A32 and PGT126 binding was evaluated. (A) Example of RNAflow FISH gating strategy based on *env* and *nef* mRNA detection. (B) Example of antibody binding among the *env/nef* mRNA– and *env/nef* mRNA+ cell population. (C) Quantification of the percentage of cells recognized by either A32 or PGT126 among the *env/nef* mRNA– and *env/nef* mRNA+ cell population with three different donors. (D–F) In a second alternative analysis, Ab-binding cells were first identified, and the HIV-infection status was then evaluated. (D) Example of flow cytometry gating strategy based on A32 or PGT126 binding. (E) Example of *env/nef* mRNA detection among the cells recognized (Ab+) or not (Ab–) by indicated mAbs. (F) Quantification of the percentage of *env/nef* mRNA+ cells among the cells recognized (Ab+) or not (Ab–) by indicated mAbs with three donors. Statistical significance was tested using a two-way ANOVA with a Holm–Sidak post-test (**P* < 0.05,***P* < 0.01, *****P* < 0.0001; ns, non-significant).

A32 does not affect HIV-1 replication or the size of HIV-1 reservoir *in vivo*

Our results indicate that nnAbs, such as A32, target nonproductively infected CD4+ T cells. It has been suggested that these cells could be in a very early stage of infection, during viral entry, before viral gene expression (86). Specifically, it has previously been shown that non-neutralizing Env epitopes, such as that targeted by A32, become transiently exposed during viral entry and could therefore represent a suitable target for ADCC at this stage (86). We hypothesized that if this was the case, then this cell population should be eliminated by A32 and therefore decrease HIV-1 replication *in vivo*. To evaluate this possibility, we tested whether A32 affected viral replication in humanized mice (hu-mice). Briefly, NOD.Cg-*Prkdc*^{scid} IL2rg$^{-/-}$ Tg(Hu-IL15) (NSG-15) hu-mice engrafted with human peripheral blood lymphocytes (hu-PBL) were infected with the primary isolate HIV-1$_{JRCSF}$ (Fig. 7A). This hu-mice model was previously shown to support HIV-1 replication and antibody Fc-effector function *in vivo* (25, 87). Infected hu-mice received nnAb A32 administered subcutaneously (S.C.) at days 6 and 9 post-infection (Fig. 7A). As controls, infected mice were also treated with the bnAbs 3BNC117 or its Fc gamma receptor (FcγR) null binding variant (GRLR) (88). Hu-mice were monitored for plasma viral loads (PVLs) and peripheral CD4+ T cells overtime (Fig. 7B and C). In the absence of antibody treatment, mice became viremic, reaching an average PVL of 2.2 × 10^7 copies/mL at day 11. As previously reported (42, 87), viral replication was associated with a loss of peripheral CD4+ T cells. Treatment with 3BNC117 (either WT or GRLR) reduced viral replication and partially restored CD4+ T cell levels in peripheral blood and several tissues. This is likely due to the neutralizing activities of both 3BNC117 variants. Although the GRLR mutations decrease FcγR binding, it does not affect the neutralizing efficacy of this antibody (88). In contrast, A32 was ineffective in reducing reduce viral replication or restoring CD4+ T cell levels (Fig. 7B through D). Interestingly, A32 treatment further

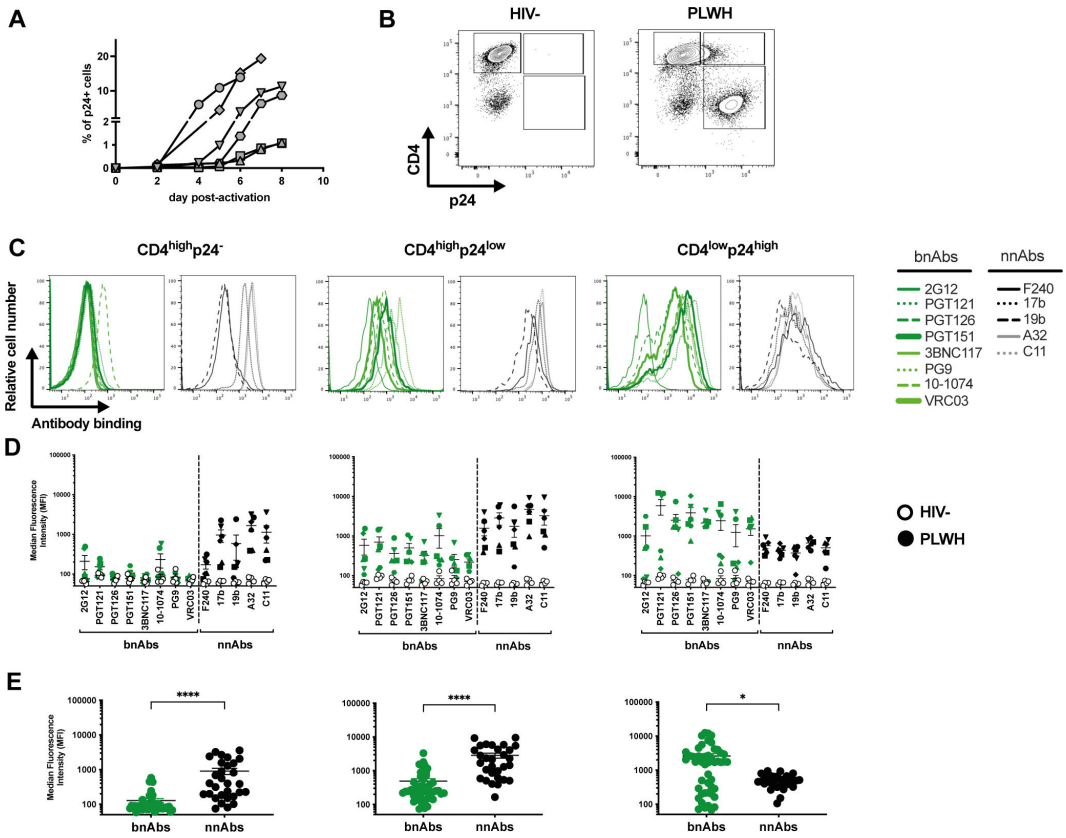

FIG 5 *Ex vivo* expanded CD4+ T cells isolated from PLWH are preferentially targeted by bNAbs. *Ex vivo* expanded CD4+ T cells from six PLWH were stained with bnAbs and nnAbs, followed by appropriate secondary Abs. Cells were then stained for surface CD4 prior to detection of intracellular HIV-1 p24. (A) Percentage of p24+ upon activation overtime. (B) Example of flow cytometry gating based on CD4 and p24 detection. (C) Histograms depicting representative staining with bnAbs (Green) and nnAbs (Black). (D) Median fluorescence intensities (MFI) obtained with primary CD4+ T cells from six PLWH. (E) Graphs shown represent the mean MFI obtained with each mAb. Each symbol represents a different HIV +donor. Statistical significance was tested using Mann–Whitney U test (*$P < 0.05$, ****$P < 0.0001$).

reduced CD4+ T cell levels in tissues relative to mock-treated mice (Fig. 7D), consistent with its capacity to recognize and eliminate uninfected bystander cells coated with soluble gp120 via ADCC (34, 74, 75). This reduction in CD4 T cell count was particularly significant when CD4+ T cell levels were considered across all tissues in mice treated with A32 nnAb alone (Fig. S7). Finally, treatment with 3BNC117 WT led to a significant reduction in the HIV-1 reservoir in multiple tissues, a phenotype not observed with A32 and not fully achieved by its FcγR null binding variant (3BNC117 GRLR, Fig. 7E). These results are in line with previous work demonstrating that bnAbs require Fc effector functions for *in vivo* activity (88). These results indicate that A32 does not reduce HIV-1 replication or the size of the reservoir in hu-mice.

DISCUSSION

ADCC represents an effective immune response involved in the clearance of virally infected cells. This adaptive immune response relies on the capacity of Abs to act as a bridge between infected cells and effector cells. While the Abs recognize infected cells through binding of surface Env via their Fab domain, their Fc domain allows the recruitment and the stimulation of FcγR bearing effector cells, leading to the killing of infected cells. ADCC-mediating Abs therefore represent attractive therapeutics for HIV cure strategies. However, the ability of Abs to recognize productively infected cells and to mediate ADCC responses depends on Env conformation (8). While bnAbs target epitopes on the prefusion "closed" Env trimer, nnAbs recognize conserved epitopes that are

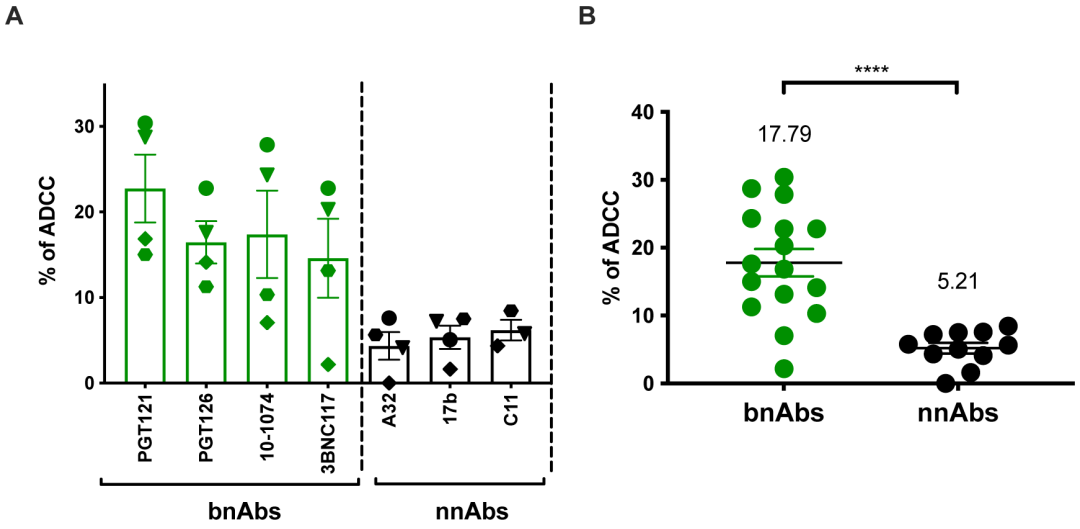

FIG 6 *Ex vivo* expanded CD4+ T cells isolated from PLWH are resistant to ADCC mediated by nnAbs. *Ex vivo* expanded CD4 T cells from PLWH were used as target cells, while autologous PBMCs were used as effector cells in our FACS-based ADCC assay. (A) Graph shown represents the percentage of ADCC against the $CD4^{low}p24^{high}$ cells with the single mAbs and (B) nnAbs vs bnAbs. (A) Each symbol represents results obtained with cells from a different PLWH. Statistical significance was tested using unpaired *t*-test (****$P < 0.0001$).

normally occluded but are exposed when Env interacts with CD4 and adopt an "open" conformation (24, 27, 30, 34–37). Here, we provide evidence that *env* mRNA expression is mainly restricted to cells that already downmodulated cell-surface CD4 (Fig. 3; Fig. S3). This prevents CD4i Env epitopes exposure on productively infected cells, thus contributing to their resistance to CD4i nnAbs.

Non-neutralizing Abs, such as those targeting the CoRBS and the inner domain of gp120 are elicited during natural infection due to exposure to "viral debris" acting as immunodominant decoy (24, 26, 29, 35, 89, 90). It is therefore not surprising that HIV-1 has evolved mechanisms to prevent surface Env–CD4 interaction to avoid Env recognition by these nnAbs, which have potent Fc-effector functions. HIV-1 utilizes Nef, Vpu, and Env to decrease cell surface CD4 on infected cells (91). Nef is expressed at high levels early during infection from a multi-spliced transcript (72, 73) and downregulates CD4 by enhancing its internalization and lysosome degradation (92–96). Vpu and Env are expressed from a Rev-depended single-spliced bicistronic mRNA later during the viral life cycle (97). Both Vpu and Env interfere with the transport of newly synthesized CD4 to the cell surface (98–100). Using RNA flow-FISH methods, we show that *env* mRNA is almost exclusively detected in cells positive for *nef* mRNA that efficiently downregulated CD4. The majority of cells expressing HIV-1 mRNA substantially downregulated surface CD4 and express high levels of p24 and Nef proteins ($CD4^{low}p24^{high}$ cells). This is consistent with previous findings demonstrating that CD4 is downmodulated from the surface of CD4 T cells positive for spliced *env* viral RNA in acutely infected PLWH (101). We also captured the stage of infection ($CD4^{low}p24^{low}$) where CD4 is already downmodulated while *env* mRNA and p24 are not fully expressed. Importantly, these cells were not efficiently recognized by either PGT126 or A32, suggesting that the Env protein is not yet fully expressed at the cell surface (Fig. S5). This suggests that Nef-mediated CD4 downmodulation precedes Env expression (Fig. 3; Fig. S3). Accordingly, productively infected cells failed to expose CD4i epitopes, explaining their resistance to ADCC mediated by nnAbs, while showing susceptibility to ADCC mediated by bNabs (Fig. 1 and 4 to 6). Furthermore, CD4 is also efficiently downregulated on the surface of latently infected cells upon reactivation with potent latency reversal agents (102), suggesting that reactivated cells should exhibit similar resistance to nnAbs-based therapy. Our findings, therefore, provide key insights for the development of immunotherapy-based cure strategies. Interestingly, a variation in bnAbs binding and ADCC was observed in *ex*

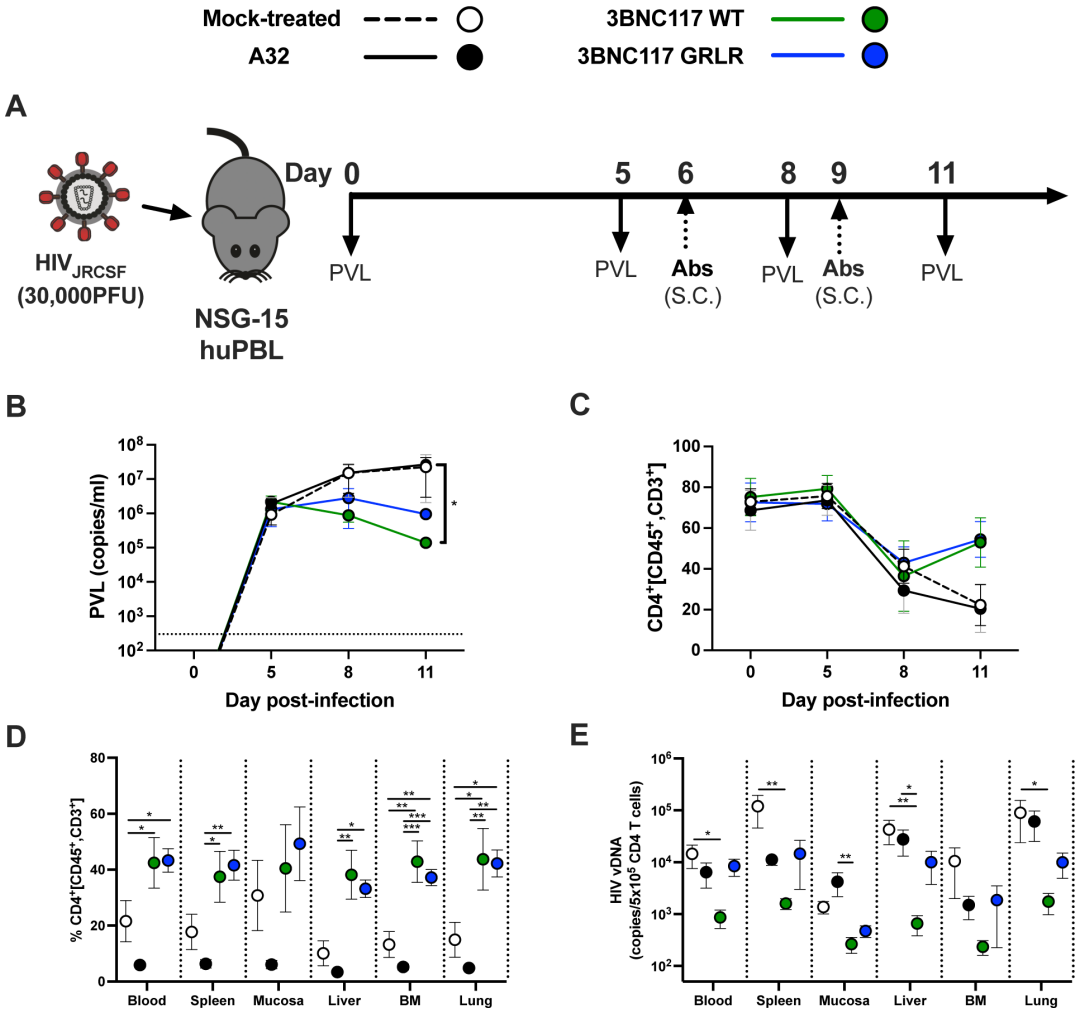

FIG 7 A32 nnAb does not impact viral replication or the size of the reservoir *in vivo*. (A) Experimental outline. NSG-15-Hu-PBL mice were infected with HIV-1 JRCSF intraperitoneally. At days 6 and 9 post infection, mice were administered 1.5 mg of A32 or 3BNC117 (WT or GRLR) mAb subcutaneously (S.C.). (B) Mice were bled routinely for plasma viral load (PVL) and flow cytometry analysis. PVL levels were measured by quantitative real-time PCR (limit of detection = 300 copies/mL, dotted line). (C) Percentage of CD4+ T cells in peripheral blood was evaluated by flow cytometry. At least six mice were used for each treatment. (D, E) Tissues of JRCSF-infected NSG-15 hu-PBL mice, treated or not with A32 or 3BNC117 (WT or GRLR), were harvested at day 11. (D) Percentage of CD4+ T cells was evaluated by flow cytometry. (E) CD4+ T cells were isolated for real-time PCR analysis of HIV DNA. Each dot represents the mean values ± SEM. S.C., subcutaneous; I.P., intraperitoneal; BM, bone marrow; mock treated, no antibody. Statistical significance was tested using one-way ANOVA with a Holm–Sidak post-test or a Kruskal–Wallis test with a Dunn's post-test (*$P < 0.05$,**$P < 0.01$,***$P < 0.001$).

vivo-expanded CD4+ T cells from PLWH relative to *in vitro*-infected cells (Fig. 1 and 5). This variation likely reflects the heterogeneity of reactivated viruses present in the PLWH samples. As bnAbs target variable regions of Env, the observed differences may be due to variations in Env sequences among the reactivated viruses. Similarly, the variability in the recognition of $CD4^{high}p24^{-}$ cells by the nnAbs could be attributed to differing levels of Env shedding by the reactivated viruses.

Our findings are also consistent with a growing number of studies demonstrating the importance of bnAbs in mediating ADCC against cells productively infected with primary HIV-1 isolates (33, 34, 36). nnAbs recognize productively infected cells only when CD4 is not completely downregulated, as is the case in infections with Nef-defective virus (Fig. 1). This is also the case when *nef*-deficient IMCs are used for ADCC detection (29, 50–61, 78, 80, 84). Most of these IMCs express the *Renilla* luciferase (LucR) reporter gene upstream of the *nef* sequence and use a T2A ribosome-skipping peptide to promote Nef expression (63). Despite documented evidence of reduced Nef expression (40, 62, 63),

these IMCs continue to be used in the ADCC field (52, 53, 55, 56, 58, 59, 103). While some studies have suggested that Vpu can compensate for the absence of Nef (52, 53), our findings refute this. Given its early expression and ability to target cell surface-expressed CD4 molecules, Nef plays the most prominent role in CD4 downmodulation (62, 91, 104). In the absence of Nef expression, we find that Vpu is not sufficient to downregulate cell-surface CD4, leading to CD4i epitope exposure and efficient nnAbs binding (Fig. 1). Other studies reporting Fc-effector functions of nnAbs employed assays unable to differentiate the ADCC responses directed against HIV-1-infected cells versus uninfected bystander cells (46, 50, 84, 105, 106). The presence of uninfected bystander cells coated with gp120 shed from productively infected cells impacts ADCC measurement by introducing a significant bias toward CD4i nnAbs (34), which is also the case when ADCC assays rely solely on target cells coated with gp120 or inactivated virions (34, 51, 61, 80, 81, 107, 108). Utilization of such assays, as well as *nef*-defective IMCs, contribute to the propagation of a misleading concept that nnAbs can effectively mediate ADCC against HIV-1-infected cells. nnAbs, such as A32, not only fail to eliminate HIV-1-infected cells but also have potentially detrimental effects by accelerating the elimination of uninfected bystander cells (34, 75), as shown in tissues of HIV-1-infected humanized mice (Fig. 7; Fig. S7). In this context, the absence of an antiviral effect of A32 in hu-mice is not surprising. Studies in non-human primate showed that elicitation of A32-like Abs by gp120 immunization or passive administration of A32 failed to confer protection against simian–human immunodeficiency virus challenges (85, 109). Similarly, a combination of anti-CoRBS and anti-cluster A (A32) nnAbs proved ineffective in delaying viral rebound after ART interruption in humanized mouse model supporting Fc effector functions (42).

The inability of A32 to recognize productively infected cells, to influence viral replication and reduce the size of reservoir in hu-mice, is a function of its epitope, which is occluded in the unliganded trimer. To our knowledge, exposure of this epitope at the surface of productively infected cells is possible in only two ways: either by membrane-bound CD4 (27) or the combination of potent small CD4-mimetic compounds (CD4mc) and anti-CoRBS Abs (28). Of note, the cocktail of A32, 17b (CoRBS Ab), and CD4mc was reported to significantly reduce the size of the reservoir in hu-mice (42).

In conclusion, we show that *env* mRNA is almost exclusively expressed by productively infected cells that downregulated cell-surface CD4. This suggests that CD4 downmodulation precedes Env expression, thus preventing exposure of vulnerable CD4-induced Env epitopes and evading ADCC mediated by nnAbs. These results must be taken into account when considering the use of nnAbs for preventative or cure strategies.

ACKNOWLEDGMENTS

The authors thank the CRCHUM BSL3 and Flow Cytometry Platforms for technical assistance, and Mario Legault from the FRQS AIDS and Infectious Diseases network for cohort coordination and clinical samples. The graphical abstract was created using BioRender.com. We thank the following collaborators for kindly providing plasmids to produce antibodies: James Robinson (Tulane University) for A32 and C11, the NIH AIDS Reagent Program for F240, 2G12 and 17b, John Mascola (Vaccine Research Center, NIAID) for VRC03, the International AIDS Vaccine Initiative (IAVI) for PG9, PGT121, PGT126, and PGT151, and Michel Nussenzweig (Rockefeller University) for 3BNC117 and 10–1074.

This study was supported by grants from the National Institutes of Health to A.F. (R01 AI148379, R01AI150322, R01AI129769, R01AI176531), P.K. (R01AI145164) and A.F. and P.K. (R01AI186809). Support for this work was also provided by P01 GM56550/AI150471 to A.F., a Canadian Institutes of Health Research (CIHR) Team grant #422148 to D.E.K, P.K., and A.F., a CIHR foundation grant #352417 to A.F. and a Canada Foundation for Innovation (CFI) grant #41027 to D.E.K. and A.F. This work was partially supported by UM1AI144462 (CHAVD) (D.E.K), UM1AI164562 (ERASE) to A.F. and P.K., and UM1AI164559 (HOPE) to P.K., and by an American Foundation for AIDS Research (amfAR) Mathilde Krim Fellowship in Basic Biomedical Research (109720–63-RKRL) to J.R. A.F. was supported by

a Canada Research Chair on Retroviral Entry #RCHS0235 950–232424. B.H.H. is supported by R01 AI162646, UM1AI144371 and UM1AI164570. J.P. was supported by a CIHR doctoral fellowship. M.B. was supported by a FRQS master's fellowship. G.B.-B. was supported by a FRQS and a CIHR doctoral fellowship. F.K. is supported by the German Research Foundation (DFG, CRC 1279) and an ERC Advanced grant (Traitor viruses). The funders had no role in study design, data collection and analysis, decision to publish, or preparation of the manuscript.

Conceptualization: J.R., G.S, L.Z, P.K., D.E.K, and A.F.; methodology: J.R., G.S, J.P., L.Z., M.D., P.K., D.E.K., and A.F.; investigation: J.R, G.S., L.Z., L.M., M.B., G.B.-B., D.C., Y.S., H.K., J.P., H.M., C.B., and G.-G.D.; resources: J.R., G.S., J.P., L.Z., L.M., M.B., G.B.-B., D.C., F.K., B.H.H., P.K., D.E.K., and A.F.; formal analysis: J.R., G.S. and L.Z.; visualization: J.R., G.S., and L.Z.; supervision: M.D., P.K., D.E.K., and A.F.; funding acquisition: J.R. P.K., D.E.K., and A.F.; writing—original draft: J.R., B.H.H., and A.F.; writing—review and editing: J.R., G.S., L.Z., J.P., L.M., M.B., G.B.-B., D.C., F.K., B.H.H., Y.S., H.K., H.M., C.B., G.-G.D., M.D., P.K., D.E.K., and A.F.

AUTHOR AFFILIATIONS

[1]Centre de Recherche du CHUM, Montréal, Québec, Canada
[2]Département de Microbiologie, Infectiologie et Immunologie, Université de Montréal, Montréal, Québec, Canada
[3]Department of Internal Medicine, Section of Infectious Diseases, Yale University School of Medicine, New Haven, Connecticut, USA
[4]Institute of Molecular Virology, Ulm University Medical Center, Ulm, Germany
[5]Department of Medicine, Perelman School of Medicine, University of Pennsylvania, Philadelphia, Pennsylvania, USA
[6]Department of Microbiology, Perelman School of Medicine, University of Pennsylvania, Philadelphia, Pennsylvania, USA
[7]Department of Medicine, Université de Montréal, Montreal, Quebec, Canada
[8]Center for HIV/AIDS Vaccine Immunology and Immunogen Discovery, The Scripps Research Institute, La Jolla, California, USA
[9]Division of Infectious Diseases, Department of Medicine, Lausanne University Hospital and University of Lausanne, Lausanne, Switzerland

AUTHOR ORCIDs

Jonathan Richard http://orcid.org/0000-0002-9015-9589
Li Zhu http://orcid.org/0000-0002-3631-1236
Frank Kirchhoff http://orcid.org/0000-0002-7052-2360
Priti Kumar http://orcid.org/0000-0002-6901-5601
Daniel E. Kaufmann http://orcid.org/0000-0003-4467-136X
Andrés Finzi http://orcid.org/0000-0002-4992-5288

DATA AVAILABILITY

Data and reagents are available upon request.

ETHICS APPROVAL

Written informed consent was obtained from all study participants, and research adhered to the ethical guidelines of CRCHUM and was reviewed and approved by the CRCHUM institutional review board (ethics committee, approval number MP-02-2024-11734). Research adhered to the standards indicated by the Declaration of Helsinki. All participants were adult and provided informed written consent prior to enrollment in accordance with Institutional Review Board approval.

ADDITIONAL FILES

The following material is available online.

Supplemental Material

Supplemental Figures (mBio01827-24-s0001.pdf). Figures S1 to S7.
Abstract (mBio01827-24-s0002.tif). Graphical abstract.

REFERENCES

1. Antiretroviral Therapy Cohort Collaboration. 2008. Life expectancy of individuals on combination antiretroviral therapy in high-income countries: a collaborative analysis of 14 cohort studies. Lancet 372:293–299. https://doi.org/10.1016/S0140-6736(08)61113-7
2. Deeks SG, Lewin SR, Havlir DV. 2013. The end of AIDS: HIV infection as a chronic disease. Lancet 382:1525–1533. https://doi.org/10.1016/S0140-6736(13)61809-7
3. Finzi D, Hermankova M, Pierson T, Carruth LM, Buck C, Chaisson RE, Quinn TC, Chadwick K, Margolick J, Brookmeyer R, Gallant J, Markowitz M, Ho DD, Richman DD, Siliciano RF. 1997. Identification of a reservoir for HIV-1 in patients on highly active antiretroviral therapy. Science 278:1295–1300. https://doi.org/10.1126/science.278.5341.1295
4. Chomont N, El-Far M, Ancuta P, Trautmann L, Procopio FA, Yassine-Diab B, Boucher G, Boulassel M-R, Ghattas G, Brenchley JM, Schacker TW, Hill BJ, Douek DC, Routy J-P, Haddad EK, Sékaly R-P. 2009. HIV reservoir size and persistence are driven by T cell survival and homeostatic proliferation. Nat Med 15:893–900. https://doi.org/10.1038/nm.1972
5. Chun TW, Stuyver L, Mizell SB, Ehler LA, Mican JA, Baseler M, Lloyd AL, Nowak MA, Fauci AS. 1997. Presence of an inducible HIV-1 latent reservoir during highly active antiretroviral therapy. Proc Natl Acad Sci U S A 94:13193–13197. https://doi.org/10.1073/pnas.94.24.13193
6. Chun TW, Carruth L, Finzi D, Shen X, DiGiuseppe JA, Taylor H, Hermankova M, Chadwick K, Margolick J, Quinn TC, Kuo YH, Brookmeyer R, Zeiger MA, Barditch-Crovo P, Siliciano RF. 1997. Quantification of latent tissue reservoirs and total body viral load in HIV-1 infection. Nat New Biol 387:183–188. https://doi.org/10.1038/387183a0
7. Checkley MA, Luttge BG, Freed EO. 2011. HIV-1 envelope glycoprotein biosynthesis, trafficking, and incorporation. J Mol Biol 410:582–608. https://doi.org/10.1016/j.jmb.2011.04.042
8. Richard J, Prévost J, Alsahafi N, Ding S, Finzi A. 2018. Impact of HIV-1 envelope conformation on ADCC responses. Trends Microbiol 26:253–265. https://doi.org/10.1016/j.tim.2017.10.007
9. Frattari GS, Caskey M, Søgaard OS. 2023. Broadly neutralizing antibodies for HIV treatment and cure approaches. Curr Opin HIV AIDS 18:157–163. https://doi.org/10.1097/COH.0000000000000802
10. Bar KJ, Sneller MC, Harrison LJ, Justement JS, Overton ET, Petrone ME, Salantes DB, Seamon CA, Scheinfeld B, Kwan RW, et al. 2016. Effect of HIV antibody VRC01 on viral rebound after treatment interruption. N Engl J Med 375:2037–2050. https://doi.org/10.1056/NEJMoa1608243
11. Caskey M, Klein F, Lorenzi JCC, Seaman MS, West AP, Buckley N, Kremer G, Nogueira L, Braunschweig M, Scheid JF, Horwitz JA, Shimeliovich I, Ben-Avraham S, Witmer-Pack M, Platten M, Lehmann C, Burke LA, Hawthorne T, Gorelick RJ, Walker BD, Keler T, Gulick RM, Fätkenheuer G, Schlesinger SJ, Nussenzweig MC. 2015. Viraemia suppressed in HIV-1-infected humans by broadly neutralizing antibody 3BNC117. Nat New Biol 522:487–491. https://doi.org/10.1038/nature14411
12. Caskey M, Schoofs T, Gruell H, Settler A, Karagounis T, Kreider EF, Murrell B, Pfeifer N, Nogueira L, Oliveira TY, et al. 2017. Antibody 10-1074 suppresses viremia in HIV-1-infected individuals. Nat Med 23:185–191. https://doi.org/10.1038/nm.4268
13. Lynch RM, Boritz E, Coates EE, DeZure A, Madden P, Costner P, Enama ME, Plummer S, Holman L, Hendel CS, et al. 2015. Virologic effects of broadly neutralizing antibody VRC01 administration during chronic HIV-1 infection. Sci Transl Med 7. https://doi.org/10.1126/scitranslmed.aad5752
14. Scheid JF, Horwitz JA, Bar-On Y, Kreider EF, Lu C-L, Lorenzi JCC, Feldmann A, Braunschweig M, Nogueira L, Oliveira T, et al. 2016. HIV-1 antibody 3BNC117 suppresses viral rebound in humans during treatment interruption. Nature New Biol 535:556–560. https://doi.org/10.1038/nature18929
15. Gaebler C, Nogueira L, Stoffel E, Oliveira TY, Breton G, Millard KG, Turroja M, Butler A, Ramos V, Seaman MS, Reeves JD, Petroupoulos CJ, Shimeliovich I, Gazumyan A, Jiang CS, Jilg N, Scheid JF, Gandhi R, Walker BD, Sneller MC, Fauci A, Chun TW, Caskey M, Nussenzweig MC. 2022. Prolonged viral suppression with anti-HIV-1 antibody therapy. Nature New Biol 606:368–374. https://doi.org/10.1038/s41586-022-04597-1
16. Mendoza P, Gruell H, Nogueira L, Pai JA, Butler AL, Millard K, Lehmann C, Suárez I, Oliveira TY, Lorenzi JCC, et al. 2018. Combination therapy with anti-HIV-1 antibodies maintains viral suppression. Nature New Biol 561:479–484. https://doi.org/10.1038/s41586-018-0531-2
17. Thali M, Moore JP, Furman C, Charles M, Ho DD, Robinson J, Sodroski J. 1993. Characterization of conserved human immunodeficiency virus type 1 gp120 neutralization epitopes exposed upon gp120-CD4 binding. J Virol 67:3978–3988. https://doi.org/10.1128/JVI.67.7.3978-3988.1993
18. Kwong PD, Wyatt R, Robinson J, Sweet RW, Sodroski J, Hendrickson WA. 1998. Structure of an HIV gp120 envelope glycoprotein in complex with the CD4 receptor and a neutralizing human antibody. Nature New Biol 393:648–659. https://doi.org/10.1038/31405
19. Wyatt R, Kwong PD, Desjardins E, Sweet RW, Robinson J, Hendrickson WA, Sodroski JG. 1998. The antigenic structure of the HIV gp120 envelope glycoprotein. Nature New Biol 393:705–711. https://doi.org/10.1038/31514
20. Tolbert WD, Gohain N, Veillette M, Chapleau JP, Orlandi C, Visciano ML, Ebadi M, DeVico AL, Fouts TR, Finzi A, Lewis GK, Pazgier M. 2016. Paring down HIV Env: design and crystal structure of a stabilized inner domain of HIV-1 gp120 displaying a major ADCC target of the A32 region. Structure 24:697–709. https://doi.org/10.1016/j.str.2016.03.005
21. Tolbert WD, Gohain N, Alsahafi N, Van V, Orlandi C, Ding S, Martin L, Finzi A, Lewis GK, Ray K, Pazgier M. 2017. Targeting the late stage of HIV-1 entry for antibody-dependent cellular cytotoxicity: structural basis for Env epitopes in the C11 region. Structure 25:1719–1731. https://doi.org/10.1016/j.str.2017.09.009
22. Gohain N, Tolbert WD, Acharya P, Yu L, Liu T, Zhao P, Orlandi C, Visciano ML, Kamin-Lewis R, Sajadi MM, Martin L, Robinson JE, Kwong PD, DeVico AL, Ray K, Lewis GK, Pazgier M. 2015. Cocrystal structures of antibody N60-I3 and antibody JR4 in complex with GP120 define more cluster a epitopes involved in effective antibody-dependent effector function against HIV-1. J Virol 89:8840–8854. https://doi.org/10.1128/JVI.01232-15
23. Gohain N, Tolbert WD, Orlandi C, Richard J, Ding S, Chen X, Bonsor DA, Sundberg EJ, Lu W, Ray K, Finzi A, Lewis GK, Pazgier M. 2016. Molecular basis for epitope recognition by non-neutralizing anti-gp41 antibody F240. Sci Rep 6:36685. https://doi.org/10.1038/srep36685
24. Veillette M, Coutu M, Richard J, Batraville LA, Dagher O, Bernard N, Tremblay C, Kaufmann DE, Roger M, Finzi A. 2015. The HIV-1 gp120 CD4-bound conformation is preferentially targeted by antibody-dependent cellular cytotoxicity-mediating antibodies in sera from HIV-1-infected individuals. J Virol 89:545–551. https://doi.org/10.1128/JVI.02868-14
25. Prévost J, Anand SP, Rajashekar JK, Zhu L, Richard J, Goyette G, Medjahed H, Gendron-Lepage G, Chen H-C, Chen Y, Horwitz JA, Grunst MW, Zolla-Pazner S, Haynes BF, Burton DR, Flavell RA, Kirchhoff F, Hahn BH, Smith AB III, Pazgier M, Nussenzweig MC, Kumar P, Finzi A. 2022. HIV-1 Vpu restricts Fc-mediated effector functions *in vivo*. Cell Rep 41:111624. https://doi.org/10.1016/j.celrep.2022.111624

26. Decker JM, Bibollet-Ruche F, Wei X, Wang S, Levy DN, Wang W, Delaporte E, Peeters M, Derdeyn CA, Allen S, Hunter E, Saag MS, Hoxie JA, Hahn BH, Kwong PD, Robinson JE, Shaw GM. 2005. Antigenic conservation and immunogenicity of the HIV coreceptor binding site. J Exp Med 201:1407–1419. https://doi.org/10.1084/jem.20042510
27. Veillette M, Désormeaux A, Medjahed H, Gharsallah N-E, Coutu M, Baalwa J, Guan Y, Lewis G, Ferrari G, Hahn BH, Haynes BF, Robinson JE, Kaufmann DE, Bonsignori M, Sodroski J, Finzi A. 2014. Interaction with cellular CD4 exposes HIV-1 envelope epitopes targeted by antibody-dependent cell-mediated cytotoxicity. J Virol 88:2633–2644. https://doi.org/10.1128/JVI.03230-13
28. Richard J, Pacheco B, Gohain N, Veillette M, Ding S, Alsahafi N, Tolbert WD, Prévost J, Chapleau J-P, Coutu M, Jia M, Brassard N, Park J, Courter JR, Melillo B, Martin L, Tremblay C, Hahn BH, Kaufmann DE, Wu X, Smith AB III, Sodroski J, Pazgier M, Finzi A. 2016. Co-receptor binding site antibodies enable CD4-mimetics to expose conserved anti-cluster a ADCC epitopes on HIV-1 envelope glycoproteins. EBioMedicine 12:208–218. https://doi.org/10.1016/j.ebiom.2016.09.004
29. Ferrari G, Pollara J, Kozink D, Harms T, Drinker M, Freel S, Moody MA, Alam SM, Tomaras GD, Ochsenbauer C, Kappes JC, Shaw GM, Hoxie JA, Robinson JE, Haynes BF. 2011. An HIV-1 gp120 envelope human monoclonal antibody that recognizes a C1 conformational epitope mediates potent antibody-dependent cellular cytotoxicity (ADCC) activity and defines a common ADCC epitope in human HIV-1 serum. J Virol 85:7029–7036. https://doi.org/10.1128/JVI.00171-11
30. Munro JB, Gorman J, Ma X, Zhou Z, Arthos J, Burton DR, Koff WC, Courter JR, Smith AB III, Kwong PD, Blanchard SC, Mothes W. 2014. Conformational dynamics of single HIV-1 envelope trimers on the surface of native virions. Science 346:759–763. https://doi.org/10.1126/science.1254426
31. Ma X, Lu M, Gorman J, Terry DS, Hong X, Zhou Z, Zhao H, Altman RB, Arthos J, Blanchard SC, Kwong PD, Munro JB, Mothes W. 2018. HIV-1 Env trimer opens through an asymmetric intermediate in which individual protomers adopt distinct conformations. Elife 7:e34271. https://doi.org/10.7554/eLife.34271
32. Herschhorn A, Ma X, Gu C, Ventura JD, Castillo-Menendez L, Melillo B, Terry DS, Smith AB III, Blanchard SC, Munro JB, Mothes W, Finzi A, Sodroski J. 2016. Release of gp120 restraints leads to an entry-competent intermediate state of the HIV-1 envelope glycoproteins. MBio 7:doi. https://doi.org/10.1128/mBio.01598-16
33. von Bredow B, Arias JF, Heyer LN, Moldt B, Le K, Robinson JE, Zolla-Pazner S, Burton DR, Evans DT. 2016. Comparison of antibody-dependent cell-mediated cytotoxicity and virus neutralization by HIV-1 ENV-specific monoclonal antibodies. J Virol 90:6127–6139. https://doi.org/10.1128/JVI.00347-16
34. Richard J, Prévost J, Baxter AE, von Bredow B, Ding S, Medjahed H, Delgado GG, Brassard N, Stürzel CM, Kirchhoff F, Hahn BH, Parsons MS, Kaufmann DE, Evans DT, Finzi A. 2018. Uninfected bystander cells impact the measurement of HIV-specific antibody-dependent cellular cytotoxicity responses. MBio 9:e00358-18. https://doi.org/10.1128/mBio.00358-18
35. Ding S, Veillette M, Coutu M, Prévost J, Scharf L, Bjorkman PJ, Ferrari G, Robinson JE, Stürzel C, Hahn BH, Sauter D, Kirchhoff F, Lewis GK, Pazgier M, Finzi A. 2016. A highly conserved residue of the HIV-1 gp120 inner domain is important for antibody-dependent cellular cytotoxicity responses mediated by anti-cluster a antibodies. J Virol 90:2127–2134. https://doi.org/10.1128/JVI.02779-15
36. Bruel T, Guivel-Benhassine F, Lorin V, Lortat-Jacob H, Baleux F, Bourdic K, Noël N, Lambotte O, Mouquet H, Schwartz O. 2017. Lack of ADCC breadth of human nonneutralizing anti-HIV-1 antibodies. J Virol 91:e02440-16. https://doi.org/10.1128/JVI.02440-16
37. Prévost J, Richard J, Ding S, Pacheco B, Charlebois R, Hahn BH, Kaufmann DE, Finzi A. 2018. Envelope glycoproteins sampling states 2/3 are susceptible to ADCC by sera from HIV-1-infected individuals. Virology (Auckl) 515:38–45. https://doi.org/10.1016/j.virol.2017.12.002
38. Alsahafi N, Ding S, Richard J, Markle T, Brassard N, Walker B, Lewis GK, Kaufmann DE, Brockman MA, Finzi A. 2015. Nef proteins from HIV-1 elite controllers are inefficient at preventing antibody-dependent cellular cytotoxicity. J Virol 90:2993–3002. https://doi.org/10.1128/JVI.02973-15
39. Richard J, Veillette M, Brassard N, Iyer SS, Roger M, Martin L, Pazgier M, Schön A, Freire E, Routy J-P, Smith AB III, Park J, Jones DM, Courter JR, Melillo BN, Kaufmann DE, Hahn BH, Permar SR, Haynes BF, Madani N, Sodroski JG, Finzi A. 2015. CD4 mimetics sensitize HIV-1-infected cells to ADCC. Proc Natl Acad Sci U S A 112:E2687–E2694. https://doi.org/10.1073/pnas.1506755112
40. Prévost J, Richard J, Medjahed H, Alexander A, Jones J, Kappes JC, Ochsenbauer C, Finzi A. 2018. Incomplete downregulation of CD4 expression affects HIV-1 Env conformation and antibody-dependent cellular cytotoxicity responses. J Virol 92:e00484-18. https://doi.org/10.1128/JVI.00484-18
41. Alsahafi N, Bakouche N, Kazemi M, Richard J, Ding S, Bhattacharyya S, Das D, Anand SP, Prévost J, Tolbert WD, Lu H, Medjahed H, Gendron-Lepage G, Ortega Delgado GG, Kirk S, Melillo B, Mothes W, Sodroski J, Smith AB III, Kaufmann DE, Wu X, Pazgier M, Rouiller I, Finzi A, Munro JB. 2019. An asymmetric opening of HIV-1 envelope mediates antibody-dependent cellular cytotoxicity. Cell Host Microbe 25:578–587. https://doi.org/10.1016/j.chom.2019.03.002
42. Rajashekar JK, Richard J, Beloor J, Prévost J, Anand SP, Beaudoin-Bussières G, Shan L, Herndler-Brandstetter D, Gendron-Lepage G, Medjahed H, et al. 2021. Modulating HIV-1 envelope glycoprotein conformation to decrease the HIV-1 reservoir. Cell Host Microbe 29:904–916. https://doi.org/10.1016/j.chom.2021.04.014
43. Laumaea A, Marchitto L, Ding S, Beaudoin-Bussières G, Prévost J, Gasser R, Chatterjee D, Gendron-Lepage G, Medjahed H, Chen H-C, Smith AB III, Ding H, Kappes JC, Hahn BH, Kirchhoff F, Richard J, Duerr R, Finzi A. 2023. Small CD4 mimetics sensitize HIV-1-infected macrophages to antibody-dependent cellular cytotoxicity. Cell Rep 42:111983. https://doi.org/10.1016/j.celrep.2022.111983
44. Herschhorn A, Gu C, Moraca F, Ma X, Farrell M, Smith AB III, Pancera M, Kwong PD, Schön A, Freire E, Abrams C, Blanchard SC, Mothes W, Sodroski JG. 2017. The β20–β21 of gp120 is a regulatory switch for HIV-1 Env conformational transitions. Nat Commun 8:1049. https://doi.org/10.1038/s41467-017-01119-w
45. Kwon YD, Finzi A, Wu X, Dogo-Isonagie C, Lee LK, Moore LR, Schmidt SD, Stuckey J, Yang Y, Zhou T, Zhu J, Vicic DA, Debnath AK, Shapiro L, Bewley CA, Mascola JR, Sodroski JG, Kwong PD. 2012. Unliganded HIV-1 gp120 core structures assume the CD4-bound conformation with regulation by quaternary interactions and variable loops. Proc Natl Acad Sci USA 109:5663–5668. https://doi.org/10.1073/pnas.1112391109
46. Alvarez RA, Hamlin RE, Monroe A, Moldt B, Hotta MT, Rodriguez Caprio G, Fierer DS, Simon V, Chen BK. 2014. HIV-1 Vpu antagonism of tetherin inhibits antibody-dependent cellular cytotoxic responses by natural killer cells. J Virol 88:6031–6046. https://doi.org/10.1128/JVI.00449-14
47. Arias JF, Heyer LN, von Bredow B, Weisgrau KL, Moldt B, Burton DR, Rakasz EG, Evans DT. 2014. Tetherin antagonism by Vpu protects HIV-infected cells from antibody-dependent cell-mediated cytotoxicity. Proc Natl Acad Sci U S A 111:6425–6430. https://doi.org/10.1073/pnas.1321507111
48. Veillette M, Coutu M, Richard J, Batraville LA, Desormeaux A, Roger M, Finzi A. 2014. Conformational evaluation of HIV-1 trimeric envelope glycoproteins using a cell-based ELISA assay. J Vis Exp 14:51995. https://doi.org/10.3791/51995:51995
49. Pauthner MG, Nkolola JP, Havenar-Daughton C, Murrell B, Reiss SM, Bastidas R, Prévost J, Nedellec R, von Bredow B, Abbink P, et al. 2019. Vaccine-induced protection from homologous tier 2 SHIV challenge in nonhuman primates depends on serum-neutralizing antibody titers. Immunity 50:241–252. https://doi.org/10.1016/j.immuni.2018.11.011
50. Bonsignori M, Pollara J, Moody MA, Alpert MD, Chen X, Hwang KK, Gilbert PB, Huang Y, Gurley TC, Kozink DM, et al. 2012. Antibody-dependent cellular cytotoxicity-mediating antibodies from an HIV-1 vaccine efficacy trial target multiple epitopes and preferentially use the VH1 gene family. J Virol 86:11521–11532. https://doi.org/10.1128/JVI.01023-12
51. Costa MR, Pollara J, Edwards RW, Seaman MS, Gorny MK, Montefiori DC, Liao HX, Ferrari G, Lu S, Wang S. 2016. Fc receptor-mediated activities of Env-specific human monoclonal antibodies generated from volunteers receiving the DNA prime-protein boost HIV vaccine DP6-001. J Virol 90:10362–10378. https://doi.org/10.1128/JVI.01458-16
52. Easterhoff D, Pollara J, Luo K, Tolbert WD, Young B, Mielke D, Jha S, O'Connell RJ, Vasan S, Kim J, et al. 2020. Boosting with AIDSVAX B/E enhances Env constant region 1 and 2 antibody-dependent cellular

cytotoxicity breadth and potency. J Virol 94:e01120-19. https://doi.org/10.1128/JVI.01120-19
53. Fisher L, Zinter M, Stanfield-Oakley S, Carpp LN, Edwards RW, Denny T, Moodie Z, Laher F, Bekker LG, McElrath MJ, Gilbert PB, Corey L, Tomaras G, Pollara J, Ferrari G. 2019. Vaccine-induced antibodies mediate higher antibody-dependent cellular cytotoxicity after interleukin-15 pretreatment of natural killer effector cells. Front Immunol 10:2741. https://doi.org/10.3389/fimmu.2019.02741
54. Huang Y, Ferrari G, Alter G, Forthal DN, Kappes JC, Lewis GK, Love JC, Borate B, Harris L, Greene K, Gao H, Phan TB, Landucci G, Goods BA, Dowell KG, Cheng HD, Bailey-Kellogg C, Montefiori DC, Ackerman ME. 2016. Diversity of antiviral IgG effector activities observed in HIV-infected and vaccinated subjects. J Immunol 197:4603–4612. https://doi.org/10.4049/jimmunol.1601197
55. Mielke D, Bandawe G, Zheng J, Jones J, Abrahams MR, Bekker V, Ochsenbauer C, Garrett N, Abdool Karim S, Moore PL, Morris L, Montefiori D, Anthony C, Ferrari G, Williamson C. 2021. ADCC-mediating non-neutralizing antibodies can exert immune pressure in early HIV-1 infection. PLoS Pathog 17:e1010046. https://doi.org/10.1371/journal.ppat.1010046
56. Mielke D, Stanfield-Oakley S, Borate B, Fisher LH, Faircloth K, Tuyishime M, Greene K, Gao H, Williamson C, Morris L, Ochsenbauer C, Tomaras G, Haynes BF, Montefiori D, Pollara J, deCamp AC, Ferrari G. 2022. Selection of HIV envelope strains for standardized assessments of vaccine-elicited antibody-dependent cellular cytotoxicity-mediating antibodies. J Virol 96:e0164321. https://doi.org/10.1128/JVI.01643-21
57. Pollara J, Bonsignori M, Moody MA, Liu P, Alam SM, Hwang KK, Gurley TC, Kozink DM, Armand LC, Marshall DJ, Whitesides JF, Kaewkungwal J, Nitayaphan S, Pitisuttithum P, Rerks-Ngarm S, Robb ML, O'Connell RJ, Kim JH, Michael NL, Montefiori DC, Tomaras GD, Liao HX, Haynes BF, Ferrari G. 2014. HIV-1 vaccine-induced C1 and V2 Env-specific antibodies synergize for increased antiviral activities. J Virol 88:7715–7726. https://doi.org/10.1128/JVI.00156-14
58. Shubin Z, Stanfield-Oakley S, Puangkaew J, Pitisutthithum P, Nitayaphan S, Gurunathan S, Sinangil F, Chariyalertsak S, Phanuphak N, Ake JA, O'Connell RJ, Vasan S, Akapirat S, Eller MA, Ferrari G, Paquin-Proulx D. 2023. Additional boosting to the RV144 vaccine regimen increased Fc-mediated effector function magnitude but not durability. AIDS 37:1519–1524. https://doi.org/10.1097/QAD.0000000000003611
59. Tuyishime M, Garrido C, Jha S, Moeser M, Mielke D, LaBranche C, Montefiori D, Haynes BF, Joseph S, Margolis DM, Ferrari G. 2020. Improved killing of HIV-infected cells using three neutralizing and non-neutralizing antibodies. J Clin Invest 130:5157–5170. https://doi.org/10.1172/JCI135557
60. Williams LD, Shen X, Sawant SS, Akapirat S, Dahora LC, Tay MZ, Stanfield-Oakley S, Wills S, Goodman D, Tenney D, et al. 2023. Viral vector delivered immunogen focuses HIV-1 antibody specificity and increases durability of the circulating antibody recall response. PLoS Pathog 19:e1011359. https://doi.org/10.1371/journal.ppat.1011359
61. Bradley T, Pollara J, Santra S, Vandergrift N, Pittala S, Bailey-Kellogg C, Shen X, Parks R, Goodman D, Eaton A, et al. 2017. Pentavalent HIV-1 vaccine protects against simian-human immunodeficiency virus challenge. Nat Commun 8:15711. https://doi.org/10.1038/ncomms15711
62. Prévost J, Richard J, Gasser R, Medjahed H, Kirchhoff F, Hahn BH, Kappes JC, Ochsenbauer C, Duerr R, Finzi A. 2022. Detection of the HIV-1 accessory proteins nef and Vpu by flow cytometry represents a new tool to study their functional interplay within a single infected CD4+ T Cell. J Virol 96:e0192921. https://doi.org/10.1128/jvi.01929-21
63. Alberti MO, Jones JJ, Miglietta R, Ding H, Bakshi RK, Edmonds TG, Kappes JC, Ochsenbauer C. 2015. Optimized replicating *Renilla* luciferase reporter HIV-1 utilizing novel internal ribosome entry site elements for native nef expression and function. AIDS Res Hum Retroviruses 31:1278–1296. https://doi.org/10.1089/aid.2015.0074
64. Sannier G, Dubé M, Dufour C, Richard C, Brassard N, Delgado G-G, Pagliuzza A, Baxter AE, Niessl J, Brunet-Ratnasingham E, Charlebois R, Routy B, Routy J-P, Fromentin R, Chomont N, Kaufmann DE. 2021. Combined single-cell transcriptional, translational, and genomic profiling reveals HIV-1 reservoir diversity. Cell Rep 36:109643. https://doi.org/10.1016/j.celrep.2021.109643
65. Baxter AE, Niessl J, Fromentin R, Richard J, Porichis F, Massanella M, Brassard N, Alsahafi N, Routy JP, Finzi A, Chomont N, Kaufmann DE. 2017. Multiparametric characterization of rare HIV-infected cells using an RNA-flow FISH technique. Nat Protoc 12:2029–2049. https://doi.org/10.1038/nprot.2017.079
66. Baxter AE, Niessl J, Fromentin R, Richard J, Porichis F, Charlebois R, Massanella M, Brassard N, Alsahafi N, Delgado GG, Routy JP, Walker BD, Finzi A, Chomont N, Kaufmann DE. 2016. Single-cell characterization of viral translation-competent reservoirs in HIV-infected individuals. Cell Host Microbe 20:368–380. https://doi.org/10.1016/j.chom.2016.07.015
67. Ochsenbauer C, Edmonds TG, Ding H, Keele BF, Decker J, Salazar MG, Salazar-Gonzalez JF, Shattock R, Haynes BF, Shaw GM, Hahn BH, Kappes JC. 2012. Generation of transmitted/founder HIV-1 infectious molecular clones and characterization of their replication capacity in CD4 T lymphocytes and monocyte-derived macrophages. J Virol 86:2715–2728. https://doi.org/10.1128/JVI.06157-11
68. van Stigt Thans T, Akko JI, Niehrs A, Garcia-Beltran WF, Richert L, Stürzel CM, Ford CT, Li H, Ochsenbauer C, Kappes JC, Hahn BH, Kirchhoff F, Martrus G, Sauter D, Altfeld M, Hölzemer A. 2019. Primary HIV-1 strains use nef to downmodulate HLA-E surface expression. J Virol 93:e00719-19. https://doi.org/10.1128/JVI.00719-19
69. Edmonds TG, Ding H, Yuan X, Wei Q, Smith KS, Conway JA, Wieczorek L, Brown B, Polonis V, West JT, Montefiori DC, Kappes JC, Ochsenbauer C. 2010. Replication competent molecular clones of HIV-1 expressing *Renilla* luciferase facilitate the analysis of antibody inhibition in PBMC. Virology (Auckl) 408:1–13. https://doi.org/10.1016/j.virol.2010.08.028
70. Adachi A, Gendelman HE, Koenig S, Folks T, Willey R, Rabson A, Martin MA. 1986. Production of acquired immunodeficiency syndrome-associated retrovirus in human and nonhuman cells transfected with an infectious molecular clone. J Virol 59:284–291. https://doi.org/10.1128/JVI.59.2.284-291.1986
71. Emi N, Friedmann T, Yee JK. 1991. Pseudotype formation of murine leukemia virus with the G protein of vesicular stomatitis virus. J Virol 65:1202–1207. https://doi.org/10.1128/JVI.65.3.1202-1207.1991
72. Klotman ME, Kim S, Buchbinder A, DeRossi A, Baltimore D, Wong-Staal F. 1991. Kinetics of expression of multiply spliced RNA in early human immunodeficiency virus type 1 infection of lymphocytes and monocytes. Proc Natl Acad Sci U S A 88:5011–5015. https://doi.org/10.1073/pnas.88.11.5011
73. Kim SY, Byrn R, Groopman J, Baltimore D. 1989. Temporal aspects of DNA and RNA synthesis during human immunodeficiency virus infection: evidence for differential gene expression. J Virol 63:3708–3713. https://doi.org/10.1128/JVI.63.9.3708-3713.1989
74. Richard J, Prévost J, Bourassa C, Brassard N, Boutin M, Benlarbi M, Goyette G, Medjahed H, Gendron-Lepage G, Gaudette F, Chen H-C, Tolbert WD, Smith AB III, Pazgier M, Dubé M, Clark A, Mothes W, Kaufmann DE, Finzi A. 2023. Temsavir blocks the immunomodulatory activities of HIV-1 soluble gp120. Cell Chem Biol 30:540–552. https://doi.org/10.1016/j.chembiol.2023.03.003
75. Richard J, Veillette M, Ding S, Zoubchenok D, Alsahafi N, Coutu M, Brassard N, Park J, Courter JR, Melillo B, Smith AB III, Shaw GM, Hahn BH, Sodroski J, Kaufmann DE, Finzi A. 2016. Small CD4 mimetics prevent HIV-1 uninfected bystander CD4 + T Cell killing mediated by antibody-dependent cell-mediated cytotoxicity. EBioMedicine 3:122–134. https://doi.org/10.1016/j.ebiom.2015.12.004
76. Brand D, Srinivasan K, Sodroski J. 1995. Determinants of human immunodeficiency virus type 1 entry in the CDR2 loop of the CD4 glycoprotein. J Virol 69:166–171. https://doi.org/10.1128/JVI.69.1.166-171.1995
77. Sloan DD, Lam C-YK, Irrinki A, Liu L, Tsai A, Pace CS, Kaur J, Murry JP, Balakrishnan M, Moore PA, Johnson S, Nordstrom JL, Cihlar T, Koenig S. 2015. Targeting HIV reservoir in infected CD4 T cells by dual-affinity re-targeting molecules (DARTs) that bind HIV envelope and recruit cytotoxic T cells. PLoS Pathog 11:e1005233. https://doi.org/10.1371/journal.ppat.1005233
78. Garrido C, Abad-Fernandez M, Tuyishime M, Pollara JJ, Ferrari G, Soriano-Sarabia N, Margolis DM. 2018. Interleukin-15-stimulated natural killer cells clear HIV-1-infected cells following latency reversal *ex vivo* J Virol 92:e00235-18. https://doi.org/10.1128/JVI.00235-18
79. Grau-Expósito J, Serra-Peinado C, Miguel L, Navarro J, Curran A, Burgos J, Ocaña I, Ribera E, Torrella A, Planas B, Badía R, Castellví J, Falcó V, Crespo M, Buzon MJ. 2017. A novel single-cell FISH-flow assay identifies effector memory CD4$^+$ T cells as a major niche for HIV-1 transcription in

HIV-infected patients. MBio 8:e00876-17. https://doi.org/10.1128/mBio.00876-17
80. Mielke D, Bandawe G, Pollara J, Abrahams MR, Nyanhete T, Moore PL, Thebus R, Yates NL, Kappes JC, Ochsenbauer C, Garrett N, Abdool Karim S, Tomaras GD, Montefiori D, Morris L, Ferrari G, Williamson C. 2019. Antibody-dependent cellular cytotoxicity (ADCC)-mediating antibodies constrain neutralizing antibody escape pathway. Front Immunol 10:2875. https://doi.org/10.3389/fimmu.2019.02875
81. Orlandi C, Flinko R, Lewis GK. 2016. A new cell line for high throughput HIV-specific antibody-dependent cellular cytotoxicity (ADCC) and cell-to-cell virus transmission studies. J Immunol Methods 433:51–58. https://doi.org/10.1016/j.jim.2016.03.002
82. Veillette M, Richard J, Finzi A. 2015. Uncovering HIV-1-infected cells. Oncotarget 6:21791–21792. https://doi.org/10.18632/oncotarget.4974
83. Astorga-Gamaza A, Grau-Expósito J, Burgos J, Navarro J, Curran A, Planas B, Suanzes P, Falcó V, Genescà M, Buzon MJ. 2022. Identification of HIV-reservoir cells with reduced susceptibility to antibody-dependent immune response. Elife 11:e78294. https://doi.org/10.7554/eLife.78294
84. Pollara J, Hart L, Brewer F, Pickeral J, Packard BZ, Hoxie JA, Komoriya A, Ochsenbauer C, Kappes JC, Roederer M, Huang Y, Weinhold KJ, Tomaras GD, Haynes BF, Montefiori DC, Ferrari G. 2011. High-throughput quantitative analysis of HIV-1 and SIV-specific ADCC-mediating antibody responses. Cytometry A 79:603–612. https://doi.org/10.1002/cyto.a.21084
85. Santra S, Tomaras GD, Warrier R, Nicely NI, Liao HX, Pollara J, Liu P, Alam SM, Zhang R, Cocklin SL, et al. 2015. Human non-neutralizing HIV-1 envelope monoclonal antibodies limit the number of founder viruses during SHIV mucosal infection in rhesus macaques. PLoS Pathog 11:e1005042. https://doi.org/10.1371/journal.ppat.1005042
86. Mengistu M, Ray K, Lewis GK, DeVico AL. 2015. Antigenic properties of the human immunodeficiency virus envelope glycoprotein gp120 on virions bound to target cells. PLoS Pathog 11:e1004772. https://doi.org/10.1371/journal.ppat.1004772
87. Abeynaike SA, Huynh TR, Mehmood A, Kim T, Frank K, Gao K, Zalfa C, Gandarilla A, Shultz L, Paust S. 2023. Human hematopoietic stem cell engrafted IL-15 transgenic NSG mice support robust NK cell responses and sustained HIV-1 infection. Viruses 15:365. https://doi.org/10.3390/v15020365
88. Bournazos S, Klein F, Pietzsch J, Seaman MS, Nussenzweig MC, Ravetch JV. 2014. Broadly neutralizing anti-HIV-1 antibodies require Fc effector functions for *in vivo* activity. Cell 158:1243–1253. https://doi.org/10.1016/j.cell.2014.08.023
89. Guan Y, Pazgier M, Sajadi MM, Kamin-Lewis R, Al-Darmarki S, Flinko R, Lovo E, Wu X, Robinson JE, Seaman MS, Fouts TR, Gallo RC, DeVico AL, Lewis GK. 2013. Diverse specificity and effector function among human antibodies to HIV-1 envelope glycoprotein epitopes exposed by CD4 binding. Proc Natl Acad Sci USA 110:E69–E78. https://doi.org/10.1073/pnas.1217609110
90. Robinson JE, Elliott DH, Martin EA, Micken K, Rosenberg ES. 2005. High frequencies of antibody responses to CD4 induced epitopes in HIV infected patients started on HAART during acute infection. Hum Antibodies 14:115–121. https://doi.org/10.3233/HAB-2005-143-408
91. Wildum S, Schindler M, Münch J, Kirchhoff F. 2006. Contribution of Vpu, Env, and Nef to CD4 down-modulation and resistance of human immunodeficiency virus type 1-infected T cells to superinfection. J Virol 80:8047–8059. https://doi.org/10.1128/JVI.00252-06
92. Piguet V, Schwartz O, Le Gall S, Trono D. 1999. The downregulation of CD4 and MHC-I by primate lentiviruses: a paradigm for the modulation of cell surface receptors. Immunol Rev 168:51–63. https://doi.org/10.1111/j.1600-065x.1999.tb01282.x
93. Bresnahan PA, Yonemoto W, Ferrell S, Williams-Herman D, Geleziunas R, Greene WC. 1998. A dileucine motif in HIV-1 Nef acts as an internalization signal for CD4 downregulation and binds the AP-1 clathrin adaptor. Curr Biol 8:1235–1238. https://doi.org/10.1016/s0960-9822(07)00517-9
94. Craig HM, Pandori MW, Guatelli JC. 1998. Interaction of HIV-1 Nef with the cellular dileucine-based sorting pathway is required for CD4 down-regulation and optimal viral infectivity. Proc Natl Acad Sci U S A 95:11229–11234. https://doi.org/10.1073/pnas.95.19.11229
95. Greenberg M, DeTulleo L, Rapoport I, Skowronski J, Kirchhausen T. 1998. A dileucine motif in HIV-1 Nef is essential for sorting into clathrin-coated pits and for downregulation of CD4. Curr Biol 8:1239–1242. https://doi.org/10.1016/s0960-9822(07)00518-0
96. Mangasarian A, Foti M, Aiken C, Chin D, Carpentier JL, Trono D. 1997. The HIV-1 Nef protein acts as a connector with sorting pathways in the Golgi and at the plasma membrane. Immunity 6:67–77. https://doi.org/10.1016/s1074-7613(00)80243-5
97. Schwartz S, Felber BK, Fenyö EM, Pavlakis GN. 1990. Env and Vpu proteins of human immunodeficiency virus type 1 are produced from multiple bicistronic mRNAs. J Virol 64:5448–5456. https://doi.org/10.1128/JVI.64.11.5448-5456.1990
98. Geleziunas R, Bour S, Wainberg MA. 1994. Cell surface down-modulation of CD4 after infection by HIV-1. FASEB J 8:593–600. https://doi.org/10.1096/fasebj.8.9.8005387
99. Willey RL, Maldarelli F, Martin MA, Strebel K. 1992. Human immunodeficiency virus type 1 Vpu protein induces rapid degradation of CD4. J Virol 66:7193–7200. https://doi.org/10.1128/JVI.66.12.7193-7200.1992
100. Willey RL, Maldarelli F, Martin MA, Strebel K. 1992. Human immunodeficiency virus type 1 Vpu protein regulates the formation of intracellular gp160-CD4 complexes. J Virol 66:226–234. https://doi.org/10.1128/JVI.66.1.226-234.1992
101. Sharma V, Creegan M, Tokarev A, Hsu D, Slike BM, Sacdalan C, Chan P, Spudich S, Ananworanich J, Eller MA, Krebs SJ, Vasan S, Bolton DL, the RV254/SEARCH010 and RV304/SEARCH013 Study Teams. 2021. Cerebrospinal fluid CD4+ T cell infection in humans and macaques during acute HIV-1 and SHIV infection. PLoS Pathog 17:e1010105. https://doi.org/10.1371/journal.ppat.1010105
102. Pardons M, Cole B, Lambrechts L, van Snippenberg W, Rutsaert S, Noppe Y, De Langhe N, Dhondt A, Vega J, Eyassu F, Nijs E, Van Gulck E, Boden D, Vandekerckhove L. 2023. Potent latency reversal by Tat RNA-containing nanoparticle enables multi-omic analysis of the HIV-1 reservoir. Nat Commun 14:8397. https://doi.org/10.1038/s41467-023-44020-5
103. Wang S, Yates NL, Pollara J, Voronin Y, Stanfield-Oakley S, Han D, Hu G, Li W, Ferrari G, Tomaras GD, Lu S. 2022. Broadly binding and functional antibodies and persisting memory B cells elicited by HIV vaccine PDPHV. NPJ Vaccines 7:18. https://doi.org/10.1038/s41541-022-00441-9
104. Chen BK, Gandhi RT, Baltimore D. 1996. CD4 down-modulation during infection of human T cells with human immunodeficiency virus type 1 involves independent activities of vpu, env, and nef. J Virol 70:6044–6053. https://doi.org/10.1128/JVI.70.9.6044-6053.1996
105. Pollara J, Orlandi C, Beck C, Edwards RW, Hu Y, Liu S, Wang S, Koup RA, Denny TN, Lu S, Tomaras GD, DeVico A, Lewis GK, Ferrari G. 2018. Application of area scaling analysis to identify natural killer cell and monocyte involvement in the GranToxiLux antibody dependent cell-mediated cytotoxicity assay. Cytometry A 93:436–447. https://doi.org/10.1002/cyto.a.23348
106. Chung AW, Navis M, Isitman G, Wren L, Silvers J, Amin J, Kent SJ, Stratov I. 2011. Activation of NK cells by ADCC antibodies and HIV disease progression. J Acquir Immune Defic Syndr 58:127–131. https://doi.org/10.1097/QAI.0b013e31822c62b9
107. Yucha R, Litchford ML, Fish CS, Yaffe ZA, Richardson BA, Maleche-Obimbo E, John-Stewart G, Wamalwa D, Overbaugh J, Lehman DA. 2023. Higher HIV-1 Env gp120-specific antibody-dependent cellular cytotoxicity (ADCC) activity is associated with lower levels of defective HIV-1 provirus. Viruses 15:2055. https://doi.org/10.3390/v15102055
108. Tomescu C, Kroll K, Colon K, Papasavvas E, Frank I, Tebas P, Mounzer K, Reeves RK, Montaner LJ. 2021. Identification of the predominant human NK cell effector subset mediating ADCC against HIV-infected targets coated with BNAbs or plasma from PLWH. Eur J Immunol 51:2051–2061. https://doi.org/10.1002/eji.202149188
109. Madani N, Princiotto AM, Mach L, Ding S, Prevost J, Richard J, Hora B, Sutherland L, Zhao CA, Conn BP, Bradley T, Moody MA, Melillo B, Finzi A, Haynes BF, Smith AB III, Santra S, Sodroski J. 2018. A CD4-mimetic compound enhances vaccine efficacy against stringent immunodeficiency virus challenge. Nat Commun 9:2363. https://doi.org/10.1038/s41467-018-04758-9